Bioorganic & Medicinal Chemistry 20 (2012) 4968–4977

Contents lists available at SciVerse ScienceDirect

Bioorganic & Medicinal Chemistry

journal homepage: www.elsevier.com/locate/bmc

Suppressive effects of coumarins from *Mammea siamensis* on inducible nitric oxide synthase expression in RAW264.7 cells

Toshio Morikawa [a], Mayumi Sueyoshi [a], Saowanee Chaipech [a], Hisashi Matsuda [b], Yukiko Nomura [b], Mikuko Yabe [b], Tomoko Matsumoto [b], Kiyofumi Ninomiya [a], Masayuki Yoshikawa [a,b], Yutana Pongpiriyadacha [c], Takao Hayakawa [a], Osamu Muraoka [a,*]

[a] Pharmaceutical Research and Technology Institute, Kinki University, 3-4-1 Kowakae, Higashi-osaka, Osaka 577-8502, Japan
[b] Kyoto Pharmaceutical University, Misasagi, Yamashina-ku, Kyoto 607-8412, Japan
[c] Faculty of Science and Technology, Rajamangala University of Technology Srivijaya, Thungsong, Nakhonsithammarat 80110, Thailand

ARTICLE INFO

Article history:
Received 10 May 2012
Revised 16 June 2012
Accepted 18 June 2012
Available online 6 July 2012

Keywords:
Mammea siamensis
Mammeasin
Coumarin
NO production inhibitor
iNOS

ABSTRACT

A methanol extract of the flowers of *Mammea siamensis* (Calophyllaceae) was found to inhibit nitric oxide (NO) production in lipopolysaccharide-activated RAW264.7 cells. From the extract, two new geranylated coumarins, mammeasins A (**1**) and B (**2**), were isolated together with 17 known compounds including 15 coumarins. The structures of **1** and **2** were determined on the basis of their spectroscopic properties as well as of their chemical evidence. Among the isolates, **1** (IC_{50} = 1.8 μM), **2** (6.4 μM), surangins B (**3**, 5.0 μM), C (**4**, 6.8 μM), and D (**5**, 6.2 μM), kayeassamins E (**7**, 6.1 μM), F (**8**, 6.0 μM), and G (**9**, 0.8 μM), mammea A/AD (**11**, 1.3 μM), and mammea E/BB (**16**, 7.9 μM) showed NO production inhibitory activity. Compounds **1**, **9**, and **11** were found to inhibit induction of inducible nitric oxide synthase (iNOS). With regard to mechanism of action of these active constituents (**1**, **9**, and **11**), suppression of STAT1 activation is suggested to be mainly involved in their suppression of iNOS induction.

1. Introduction

Mammea siamensis (Miq.) T. Anders. (Calophyllaceae), known in Thai as "Sarapi", is a small evergreen tree distributed in Thailand, Laos, Cambodia, Vietnam, and Myanmar, etc. The flowers of this plant have been used for a heart tonic in Thai traditional medicine.[1–7] By previous chemical studies on the flowers,[2,3,8,9] seeds,[4,6] twigs,[1,5] and barks[7] of *M. siamensis*, presence of several coumarins,[2,4,5,7–9] xanthones,[1,6] triterpenoids,[3] and steroids[3] have been revealed. In the course of our characterization studies on bioactive constituents in Thai natural medicines,[10–27] the methanol extract of the flowers of *M. siamensis* was found to inhibit nitric oxide (NO) production in lipopolysaccharide (LPS)-activated RAW264.7 cells. By bioassay-guided separation, two new geranylated coumarins, mammeasins A (**1**) and B (**2**), were isolated together with 17 known compounds including 15 coumarins (**3–17**). This paper deals with the isolation and structural elucidation of these new geranylated coumarins (**1** and **2**) as well as inhibitory effects of the coumarin constituents on the LPS-activated NO production. Furthermore, to clarify the mechanism of action of the NO production inhibitory activity, effects of three active coumarins (**1**, **9**, and **11**) on protein levels of inducible NO synthase (iNOS), activation of mitogen-activated protein kinases (MAPK) [c-Jun N-terminal kinase (JNK) and p38], and nuclear protein levels of phosphorylated signal transducer and activator of transcription-1 (STAT1) (p-STAT1) as well as nuclear factor κ-B (NF-κB) were examined.

2. Results and discussion

2.1. Effect of methanol extract from the flowers of *M. siamensis* on NO production in LPS-activated RAW264.7 cells

The dried flowers of *M. siamensis* (collected in Nakhonsithammarat Province, Thailand) were extracted with methanol under reflux to yield a methanolic extract (25.66% from the dried flower). The methanol extract was partitioned into an EtOAc–H_2O (1:1, v/v) mixture to furnish an EtOAc-soluble fraction (6.84%) and an aqueous phase. The aqueous phase was subjected to Diaion HP-20 column chromatography ($H_2O \rightarrow$ MeOH) to give H_2O- and MeOH-eluted fractions (13.50% and 4.22%, respectively). As shown in Table 1, the methanol extract was found to inhibit LPS-activated NO production in RAW264.7 cells (IC_{50} = 28.9 μg/mL). By bioassay-guided fractionation, the EtOAc-soluble fraction was found to be the active fraction (IC_{50} = 8.3 μg/mL), although the fraction exhibited cytotoxic effects in MTT assay. On the other hand, the MeOH- and H_2O-eluted fractions showed no activity.

* Corresponding author. Tel.: +81 6 6721 2332; fax: +81 6 6729 3577.
E-mail address: muraoka@phar.kindai.ac.jp (O. Muraoka).

0968-0896/$ - see front matter © 2012 Elsevier Ltd. All rights reserved.
http://dx.doi.org/10.1016/j.bmc.2012.06.031

Table 1
Inhibitory effects of the methanolic extract and its fractions from the flowers of *M. siamensis* on LPS-activated NO production in RAW264.7 cells

	Inhibition (%)[a]				IC_{50} (μg/mL)
	0 μg/mL	10 μg/mL	30 μg/mL	100 μg/mL	
MeOH extract	0.0 ± 1.9	38.1 ± 1.4[b]	55.7 ± 0.8[b]	64.6 ± 0.7[b] (86.7 ± 1.7)	28.9
EtOAc-soluble fraction	0.0 ± 1.4	60.4 ± 0.9[b]	65.0 ± 1.9[b,c] (45.8 ± 1.6)	95.8 ± 0.2[b,c] (27.3 ± 1.1)	8.3
MeOH-eluted fraction	0.0 ± 4.2	3.5 ± 3.7	7.8 ± 1.3	15.2 ± 1.5[b]	>100
H_2O-eluted fraction	0.0 ± 1.4	5.0 ± 0.8	7.6 ± 0.9	−1.7 ± 1.7	>100

[a] Each value represents the mean ± SEM ($N = 4$).
[b] Significantly different from the control, $p < 0.01$.
[c] Cytotoxic effects were observed, and values in parentheses indicate cell viability (%) in MTT assay.

2.2. Chemical constituents from the flowers of *M. siamensis*

The EtOAc-soluble fraction was subjected to silica gel and ODS column chromatography and finally HPLC to furnish mammeasins A (**1**, 0.0293% from the dried flower) and B (**2**, 0.0123%). Additionally, 15 coumarins, surangins B[4,28–30] (**3**, 0.0337%), C[31,32] (**4**, 0.0571%), and D[7] (**5**, 0.0632%), kayeassamins A[33] (**6**, 0.0578%), E[34] (**7**, 0.0113%), F[34] (**8**, 0.0390%), and G[34] (**9**, 0.0171%), mammea A/AC[35,36] (**10**, 0.0555%), mammea A/AD[37] (**11**, 0.0022%), mammea A/AB cyclo D[38] (**12**, 0.0047%), mammea A/AC cyclo D[35] (**13**, 0.0077%), mammea B/AB cyclo D[37,38] (**14**, 0.0016%), mammea B/AC cyclo D[8] (**15**, 0.0055%), mammea E/BB[4,39] (**16**, 0.0194%), and deacetylmammea E/BC cyclo D[9] (**17**, 0.0073%), and β-amyrin[40] (0.0072%) and benzoic acid[40] (0.0043%) were isolated from this plant material (Fig. 1).

2.3. Structures of mammeasins A (1) and B (2)

Mammeasin A (**1**) was obtained as a pale yellow oil with negative optical rotation ($[\alpha]_D^{27}$ −25.4 in $CHCl_3$). Its IR spectrum showed absorption bands at 3503, 1748, 1717, and 1609 cm^{-1} ascribable to hydroxyls, ester carbonyl, α,β-unsaturated γ-lactone, and chelated acyl groups. The UV spectrum exhibited absorption

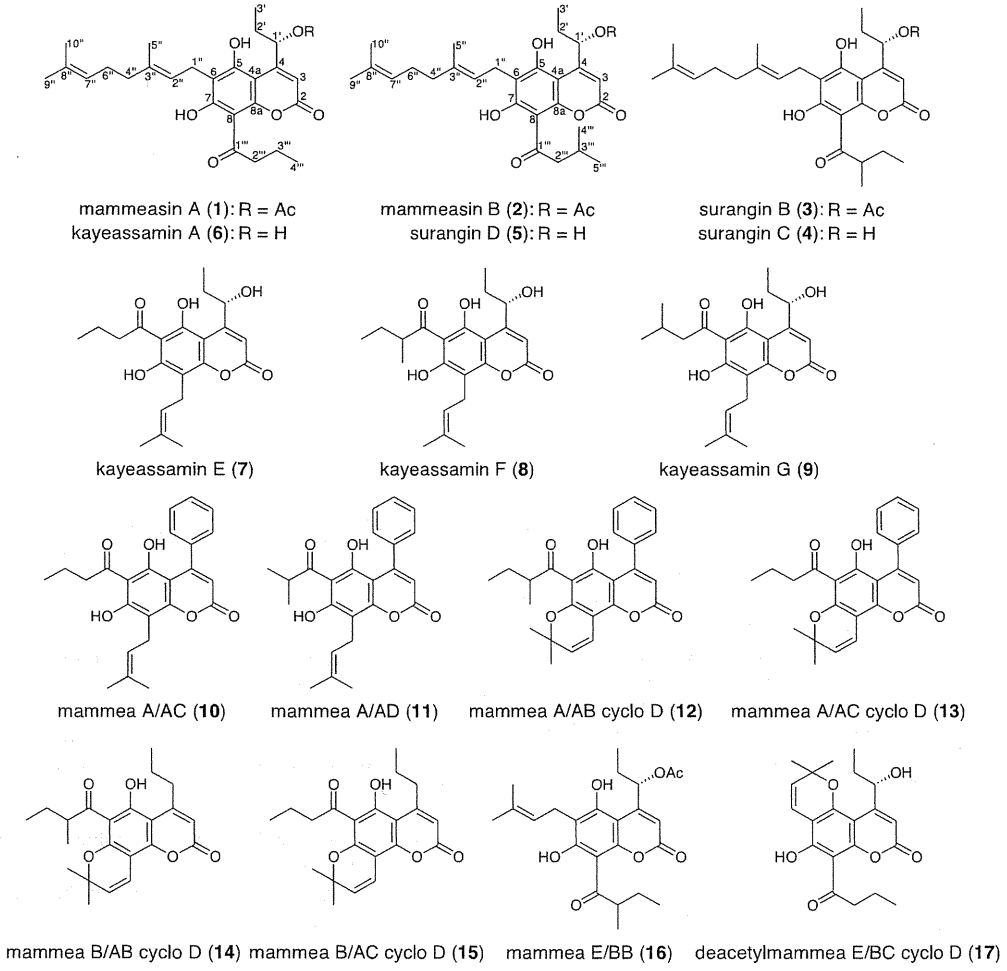

Figure 1. Coumarin constituents (**1–17**) from the flowers of *M. siamensis*.

Table 2
^{1}H NMR (700 MHz, $CDCl_3$) data on mammeasins A (**1**) and B (**2**)

Position	**1** δ_H (*J*, Hz)	**2** δ_H (*J*, Hz)
3	6.27 (1H, d, 1.1)	6.27 (d, 1.1)
1′	6.48 (1H, ddd, 1.1, 2.4, 8.0)	6.48 (1H, ddd, 1.1, 2.6, 7.9)
2′	1.68 (1H, m)	1.68 (1H, m)
	1.95 (1H, ddq, 2.4, 14.4, 7.2)	1.95 (1H, m)
3′	1.00 (3H, dd, 7.2, 7.2)	1.00 (3H, dd, 7.2, 7.2)
1″	3.48 (1H, dd, 7.4, 16.5)	3.48 (1H, dd, 7.2, 16.7)
	3.51 (1H, dd, 7.0, 16.5)	3.52 (1H, dd, 7.4, 16.7)
2″	5.24 (1H, ddq, 7.0, 7.4, 1.0)	5.25 (1H, ddq, 7.0, 7.2, 1.0)
4″	2.11 (2H, m)	2.12 (2H, m)
5″	1.86 (3H, d, 1.0)	1.86 (3H, br s)
6″	2.11 (2H, m)	2.12 (2H, m)
7″	5.06 (1H, m)	5.06 (1H, m)
9″	1.68 (3H, s)	1.68 (3H, s)
10″	1.60 (3H, d, 0.8)	1.60 (3H, d, 0.8)
2‴	3.27 (2H, t, 7.2)	3.12 (1H, dd, 6.6, 15.9)
		3.17 (1H, dd, 6.6, 15.9)
3‴	1.78 (2H, tq, 7.2, 7.4)	2.27 (1H, m)
4‴	1.04 (3H, t, 7.4)	1.03 (3H, d, 6.7)
5‴		1.03 (3H, d, 6.7)
1″-*OAc*	2.18 (3H, s)	2.18 (3H, s)
7-*OH*	14.69 (1H, s)	14.67 (1H, s)

maxima at 223 and 330 nm, similar to those of 5,7-dioxygenated coumarins.[5,33,34,37] The EIMS spectrum of **1** showed a molecular ion peak at *m/z* 484 (M^+), and the molecular formula was determined as $C_{28}H_{36}O_7$ by high-resolution EIMS measurement. The ^{1}H and ^{13}C NMR spectra of **1** ($CDCl_3$, Tables 2 and 3), which were assigned by means of various NMR experiments,[41] showed signals assignable to two primary and three vinyl methyls [δ 1.00 (3H, dd, J = 7.2, 7.2 Hz, H_3-3′), 1.04 (3H, t, J = 7.4 Hz, H_3-4‴), 1.60 (3H, d, J = 0.8 Hz, H_3-10″), 1.68 (3H, s, H_3-9″), 1.86 (3H, d, J = 1.0 Hz, H_3-5″)], six methylenes {δ [1.68 (1H, m), 1.95 (1H, ddq, J = 2.4, 14.4, 7.2 Hz), H_2-2′], 1.78 (2H, tq, J = 7.2, 7.4 Hz, H_2-3‴), 2.11 (4H, m, H_2-4″, 6″), 3.27 (2H, t, J = 7.2 Hz, H_2-2‴), [3.48 (1H, dd, J = 7.4, 16.5 Hz), 3.51 (1H, dd, J = 7.0, 16.5 Hz), H_2-1″]}, a methine bearing an oxygen function [δ 6.48 (1H, ddd, J = 1.1, 2.4, 8.0 Hz, H-1′)], and three olefinic protons [δ 5.06 (1H, m, H-7″), 5.24 (1H, ddq, J = 7.0, 7.4, 1.0 Hz, H-2″), 6.27 (1H, d, J = 1.1 Hz, H-3)] together with an acetyl group [δ 2.18 (3H, s); δ_C 21.1, 170.4]. The ^{1}H and ^{13}C NMR spectroscopic properties of **1** were quite similar to those of **6**, except for the signal due to the acetyl group. The ^{1}H–^{1}H COSY experiment on **1** indicated the presence of partial structures shown in bold lines in Figure 2. In the HMBC experiment, long-range correlations were observed between the following proton and carbon pairs (H-3 and C-2, 4a, 1′; H-1′ and C-3, 4a, 1′-$OCOCH_3$; H_2-1″ and C-5–7; H-2″ and C-6, 3″, 5″; H_2-4″ and C-3″; H_2-7″ and C-9″, 10″; H_3-5″ and C-2″–4″; H_3-9″ and C-7″, 8″, 10″; H_3-10″ and C-7″–9″; H_2-2‴ and C-1‴). In order to elucidate the absolute stereostructure, **1** was chemically related to **6**, for which the absolute configuration at the C-1′ was reported.[33] As shown in Figure 3, acetylation of **6** with acetic anhydride (Ac_2O) in pyridine furnished **1**, so that the absolute configuration at the C-1′ was determined to be *S* orientation.

Table 3
^{13}C NMR (175 MHz, $CDCl_3$) data on mammeasins A (**1**) and B (**2**)

Position	**1** δ_C	**2** δ_C
2	159.5	159.4
3	106.4	106.4
4	157.3	157.1
4a	100.4	100.4
5	158.3	158.3
6	110.2	110.2
7	165.7	165.7
8	104.6	104.6
8a	156.2	156.2
1′	73.7	73.7
2′	28.7	28.7
3′	10.1	10.1
1″	21.6	21.6
2″	120.0	119.7
3″	142.6	142.5
4″	39.7	39.7
5″	16.5	16.5
6″	26.4	26.4
7″	123.3	123.3
8″	132.3	132.3
9″	25.7	25.6
10″	17.7	17.7
1‴	206.5	206.3
2‴	46.8	53.6
3‴	18.1	25.6
4‴	13.8	22.6
5‴		22.6
1′-OAc	170.4	170.3
	21.1	21.0

Mammeasin B (**2**) was also isolated as a pale yellow oil with negative optical rotation ($[\alpha]_D^{26}$ −18.4 in $CHCl_3$). The EIMS of **2** showed a molecular ion peak at *m/z* 498 (M^+), and the molecular formula was determined as $C_{29}H_{38}O_7$, by high-resolution EIMS measurement. The ^{1}H and ^{13}C NMR spectroscopic properties of **2** were similar to those of **1**, and showed signals assignable to a primary, two secondary, and three vinyl methyls [δ 1.00 (3H, dd, J = 7.2, 7.2 Hz, H_3-3′), 1.03 (6H, d, J = 6.7 Hz, H_3-4‴, 5‴), 1.60 (3H, d, J = 0.8 Hz, H_3-10″), 1.68 (3H, s, H_3-9″), 1.86 (3H, br s, H_3-5″)], five methylenes {δ 1.68, 1.95 (1H each, m, H_2-2′), 2.12 (4H, m, H_2-4″, 6″), 3.12, 3.17 (1H each, both dd, J = 6.6, 15.9 Hz, H_2-2‴), [3.48 (1H, dd, J = 7.2, 16.7 Hz), 3.52 (1H, dd, J = 7.4, 16.7 Hz), H_2-1″]}, a methine [δ 2.27 (1H, m, H-3‴)], a methine bearing an oxygen function [δ 6.48 (1H, ddd, J = 1.1, 2.6, 7.9 Hz, H-1′)], and three olefinic protons [δ 5.06 (1H, m, H-7″), 5.25 (1H, ddq, J = 7.0, 7.2, 1.0 Hz, H-2″), 6.27 (1H, d, J = 1.1 Hz, H-3)] together with an acetyl group [δ 2.18 (3H, s); δ_C 21.0, 170.3]. The ^{1}H and ^{13}C NMR spectroscopic properties of **2** were superimposable on those of **5**, except for the singals due to the acetyl group. As shown in Figure 2, the connectivity of the acetyl group in **2** was elucidated on the basis of the ^{1}H–^{1}H COSY and HMBC experiments. In addition, **2** was obtained by acetylation of **5** as shown in Figure 3. Thus, the planar structure of **2** was characterized to be as shown. Since the absolute stereochemistry of **5** has been uncharacterized, the absolute configuration of the C-1′ position in **5** was determined in the present study by the modified Mosher's method.[42] Thus, **5** was derived to the corresponding MTPA esters, 1′-(*R*)-MTPA ester (**5a**) and 1′-(*S*)-MTPA ester (**5b**), by treatment with (*S*)-(+)-α-methoxy-α-(trifluoromethyl)phenylacetic chloride [(*S*)-(+)-MTPA-Cl] and its (*R*)-isomer, respectively, in pyridine. As shown in Figure 3, signal due to the proton at C-3 in **5b** was observed at lower field compared with that of **5a** [$\Delta\delta$: positive], while the signals due to protons at C-2′ and C-3′ in **5b** were observed at higher field compared with those of **5a** [$\Delta\delta$: negative]. Thus, the absolute configuration at C-1′ of **5** was determined to be *S* orientation. Consequently, the absolute stereostructures of **2** and **5** were elucidated to be as shown in Figure 3.

2.4. Inhibitory effects on LPS-activated NO production in RAW264.7 cells

Inflammation is a systemic response aimed to decrease the toxicity of harmful agents and repair damaged tissue.[43] A key feature

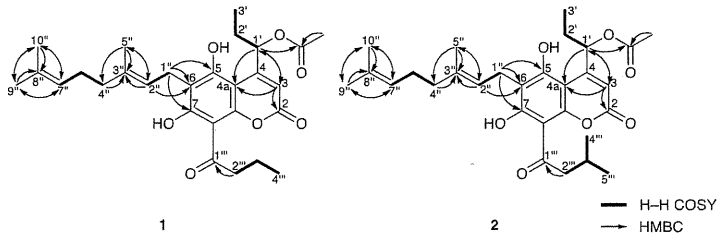

Figure 2. ^{1}H–^{1}H COSY and HMBC correlations of **1** and **2**.

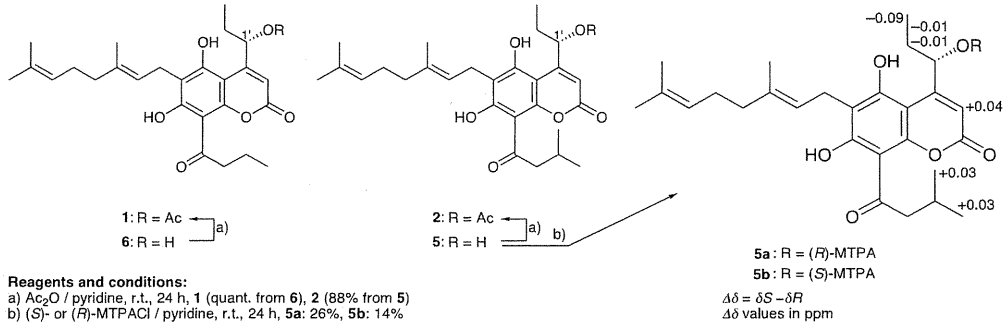

Figure 3. Absolute stereostructures of **1**, **2**, and **5**.

of the inflammatory response is the activation of phagocytic cells involved in host defense, which produce an oxidative burst of reactive oxygen, chlorine, and nitrogen species.[43,44].

Macrophages play major roles in the immunity and inflammatory responses involved in host defense. Once activated, they initiate the production of cytokines, oxygen and nitrogen species, and eicosanoids. In macrophages, bacterial lipopolysaccharide (LPS) is best able to induce the transcription of genes encoding pro-inflammatory proteins. The stimulation results in the release of cytokines and synthesis of enzymes such as inducible nitric oxide synthase (iNOS). The nitric oxide (NO) radical is known to play a central role in inflammatory and immune reactions.[45,46] It is synthesized through the L-arginine pathway by three types of nitric oxide synthase (NOS): endothelial NOS (eNOS), neural NOS (nNOS) and iNOS.[47,48] eNOS and nNOS are constitutively expressed at low levels. Under normal physiological conditions, iNOS is dormant in resting cells, but under pathological conditions, it produces a large amount of NO leading to a 10-fold higher level of eNOS by interferon-γ (IFNγ) and LPS[49,50] and plays a dual role in chronic infection, inflammation and carcinogenesis.[48,51] As a part of our studies to characterize the bioactive components of natural medicines, we have investigated various NO production inhibitors.[10,52–59]

Table 4
Inhibitory effects of the constituents from the flowers of *M. siamensis* on LPS-activated NO production in RAW264.7 cells

	Inhibition (%)[a]					IC_{50} (μM)
	0 μM	1 μM	3 μM	10 μM	30 μM	
Mammeasin A (**1**)	0.0 ± 1.3	27.5 ± 2.4[b]	72.9 ± 10.5[b,c] (56.4 ± 1.9)	88.1 ± 0.9[b,c] (24.1 ± 0.8)	92.0 ± 1.0[b,c] (10.2 ± 0.1)	1.8
Mammeasin B (**2**)	0.0 ± 2.0	0.6 ± 2.9	31.1 ± 6.7[b,c] (60.3 ± 2.4)	64.7 ± 2.2[b,c] (20.2 ± 0.8)	88.2 ± 1.4[b,c] (13.6 ± 0.4)	6.4
Surangin B (**3**)	0.0 ± 1.5	8.5 ± 0.5	35.7 ± 0.6[b,c] (67.1 ± 4.3)	74.3 ± 0.7[b,c] (42.3 ± 1.2)	91.1 ± 1.1[b,c] (18.1 ± 0.4)	5.0
Surangin C (**4**)	0.0 ± 2.9	18.1 ± 0.7[b]	40.8 ± 1.6[b]	56.7 ± 0.8[b,c] (61.7 ± 0.9)	71.3 ± 0.6[b,c] (42.9 ± 0.8)	6.8
Surangin D (**5**)	0.0 ± 1.4	22.7 ± 0.3[b]	41.1 ± 0.8[b]	55.4 ± 1.0[b]	74.0 ± 0.8[b] (104.5 ± 3.4)	6.2
Kayeassamin A (**6**)	0.0 ± 2.0	5.0 ± 4.7	15.0 ± 1.4[b]	29.7 ± 1.8[b]	56.6 ± 1.2[b] (82.4 ± 1.3)	26.6
Kayeassamin E (**7**)	0.0 ± 0.7	38.7 ± 1.0[b]	38.8 ± 0.2[b]	67.1 ± 0.6[b,c] (42.8 ± 2.3)	63.8 ± 1.6[b,c] (42.2 ± 1.3)	6.1
Kayeassamin F (**8**)	0.0 ± 2.6	31.4 ± 0.6[b]	41.3 ± 1.0[b]	60.7 ± 1.8[b,c] (55.2 ± 2.4)	63.1 ± 1.0[b,c] (31.5 ± 0.9)	6.0
Kayeassamin G (**9**)	0.0 ± 1.9	51.0 ± 0.6[b]	55.9 ± 1.2[b]	81.5 ± 0.6[b,c]	72.3 ± 0.3[b,c] (83.7 ± 1.2)	0.8
Mammea A/AC (**10**)	0.0 ± 14.9	0.6 ± 1.9	14.2 ± 3.0	46.9 ± 5.3[b]	67.6 ± 0.9[b] (96.8 ± 1.7)	13.0
Mammea A/AD (**11**)	0.0 ± 1.5	33.7 ± 2.1[b]	83.4 ± 0.8[b,c] (57.2 ± 0.9)	89.4 ± 0.8[b,c] (27.2 ± 0.9)	102.6 ± 0.4[b,c] (10.1 ± 0.5)	1.3
Mammea A/AB cyclo D (**12**)	0.0 ± 1.3			12.9 ± 1.0[b]	18.3 ± 1.1[b]	>30
Mammea A/AC cyclo D (**13**)	0.0 ± 1.7			9.4 ± 1.4	14.3 ± 0.8[b]	>30
Mammea B/AB cyclo D (**14**)	0.0 ± 0.5			10.6 ± 0.5[b]	13.3 ± 1.5[b]	>30
Mammea B/AC cyclo D (**15**)	0.0 ± 0.7			9.9 ± 0.4[b]	13.8 ± 0.5[b]	>30
Mammea E/BB (**16**)	0.0 ± 1.1	−1.5 ± 1.4	24.2 ± 2.0[b,c] (55.3 ± 3.2)	50.5 ± 1.1[b,c] (29.9 ± 2.3)	89.1 ± 0.3[b,c] (11.0 ± 0.3)	7.9
Deacetylmammea E/BC cyclo D (**17**)	0.0 ± 2.4	15.1 ± 1.9	20.2 ± 2.5[b]	33.1 ± 2.0[b]	62.3 ± 1.1[b] (106.9 ± 4.8)	19.7
SB202190	0.0 ± 2.6			36.8 ± 1.7[b]	70.2 ± 0.3[b] (81.4 ± 1.7)	ca. 16
CAPE[59]	0.0 ± 0.7	5.4 ± 2.0	45.7 ± 3.2[b]	98.4 ± 0.8[b,c] (76.4 ± 6.1)	100.3 ± 0.1[b,c] (15.6 ± 0.7)	3.8

[a] Each value represents the mean ± SEM ($N = 4$).
[b] Significantly different from the control, $p < 0.01$.
[c] Cytotoxic effects were observed, and values in parentheses indicate cell viability (%) in MTT assay.

As a continuation of these studies on bioactive constituents of natural medicines, the effects of the coumarin constituents (**1**–**17**) from the flowers of *M. siamensis* on NO production from LPS-activated RAW264.7 cells were examined, and the results were summarized in Table 4. As the result, compounds **1**–**11**, **16**, and **17** showed NO production inhibitory activities (IC_{50} = 0.8–26.6 μM), although half of them (**1**, **2**, **3**, **4**, **7**, **8**, **11**, and **16**) showed considerable cytotoxic effects even at low concentrations in the MMT assays. Among the active compounds, kayeassamin G (**9**) was found to be the most potent, and strongly inhibited the production of NO (IC_{50} 0.8 μM) without notable cytotoxic effects at the effective concentrations (<10 μM). Whereas mammeasin A (**1**, IC_{50} = 1.8 μM) and mammea A/AD (**11**, 1.3 μM) showed considerable cytotoxic effects although they inhibited the NO production to the same extent as **9**. It is noteworthy that the hydroxyl at C-7 was essential for the strong activity. Once the hydroxyl was masked as the 2,2-dimethylchromene moiety (**12**–**15**), they significantly lost the activity. With respect to the substituents at C-4, C-6, and C-8, no distinct relationships were detected between the structures and the activity in the present study. Regardless of the structure of the substituents, all the tested compounds bearing the C-7 hydroxyl showed a certain degree of activity.

2.5. Inhibitory mechanism of 1, 9, and 11 on iNOS induction

NF-κB is a major transcription factor involved in iNOS and TNF-α gene expression. NF-κB is present as an inactive form due to combination with an inhibitory subunit, IκB, which keeps NF-κB in the cytoplasm, thereby preventing activation of the target gene in the nucleus. Cellular signals lead to phosphorylation of IκB following elimination of IκB from NF-κB by proteolytic degradation. Then, the activated-NF-κB is released and translocated into the nucleus to activate transcription of its target genes.[60] Inhibition of iNOS enzyme activity or iNOS induction and inhibition of NF-κB activation may be of therapeutic benefit in various types of inflammation.[48–51,61]

First, the effects of three coumarins (**1**, **9**, and **11**) on iNOS induction were examined. iNOS was detected at 130 kDa after a 20-h incubation with LPS by sodium dodecylsulfate–polyacrylamide gel electrophoresis (SDS–PAGE)–Western blot analysis. As shown in Figure 4, iNOS induction in LPS-activated RAW264.7 cells was suppressed by **1**, **9**, and **11**, and it was closely related to their inhibitions of NO production. These results suggested that the three coumarins (**1**, **9**, and **11**) inhibited NO production due to their inhibitory activities against iNOS induction in LPS-activated RAW264.7 cells. However, the NF-κB levels in a nuclear protein fraction were not reduced by **1**, **9**, and **11** (Fig. 5). Therefore, other mechanisms of action were suggested to exist.

The MAPK superfamily of serine/threonine kinases is an important component of cellular signal transduction and also appears to play important roles in inflammatory processes. At least, three MAPK cascades; extracellular signal-regulated kinase (ERK), JNK, and p38 are involved in inflammation.[62–64] Recently, inhibitors of the phosphorylation of JNK, but not of ERK, were reported to reduce LPS-stimulated NO production.[65] In contrast, Hwang et al. reported that the inhibitors of phosphorylation of ERK and p38, but not of JNK, reduced LPS-stimulated NO production.[66] In our previous study,[58] a MAPK-ERK kinase 1 (MEK1) inhibitor (PD98059) acting on the phosphorylation of ERK and an ERK inhibitor (FR180204) showed less inhibition against the production of NO;

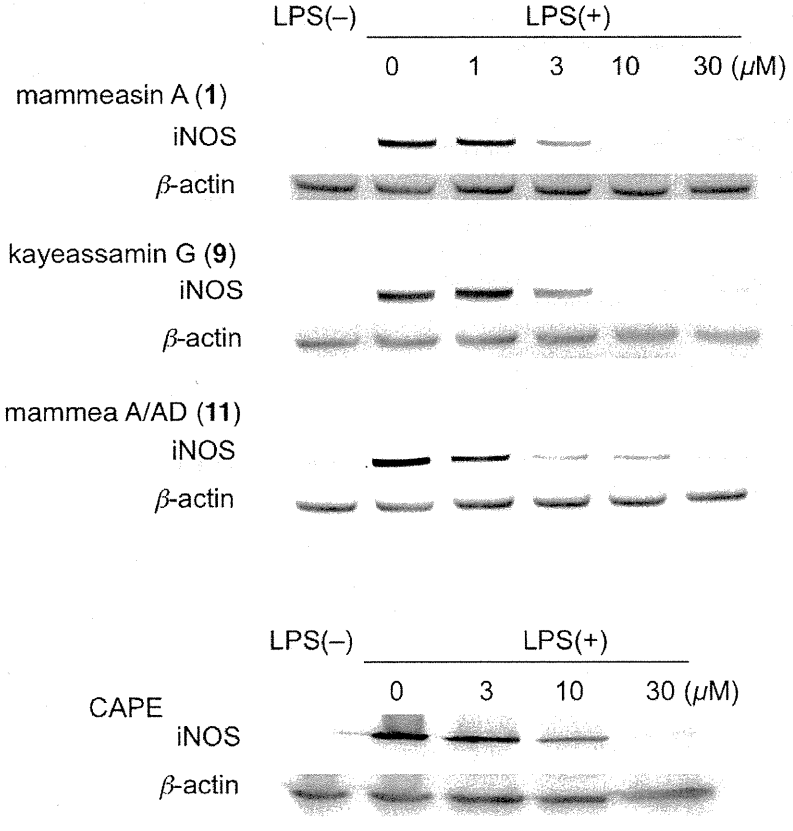

Figure 4. Effects of **1**, **9**, **11**, and CAPE on iNOS protein levels.

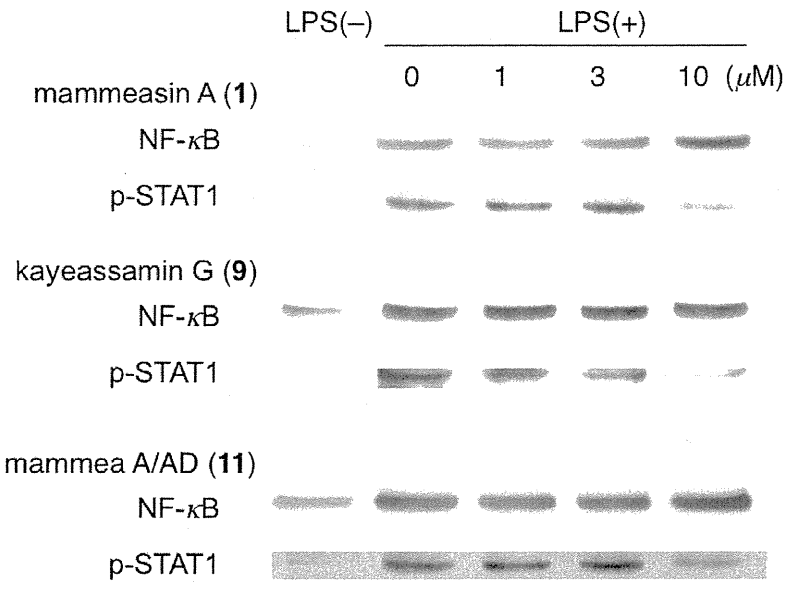

Figure 5. Effects of **1**, **9**, and **11** on nuclear protein levels of NF-κB and p-STAT1.

−2.4 ± 1.1% inhibition at 100 μM and 7.2 ± 2.2% inhibition at 10 μM, respectively. While a JNK inhibitor (SP600125) significantly inhibited the production of NO (74.6 ± 0.6% inhibition at 30 μM, IC_{50} = 17 μM) consistent with the previous report by Lin et al.[65] Furthermore, an inhibitor of phosphorylation of p38, SB202190, showed significant inhibition (IC_{50} = ca. 16 μM) (Table 4). These findings suggested that phosphorylations of JNK and p38 are important steps for expression of iNOS under our experimental conditions. However, in the present study, the active coumarins (**1**, **9**, and **11**) did not inhibit the phosphorylations of these MAP kinases (Fig. 6).

Signal transducer and activator of transcription-1 (STAT1) as well as NF-κB are also important nuclear factor for iNOS expression, and STAT1 is known to activate by IFNβ or IFNγ. Transcription of IFNβ by LPS via Toll-like receptor-4 (TLR4) is reported to be independent of activation of NF-κB, but LPS induce the IFNβ via activation of IFN-regulatory factor-3 (IRF3) in macrophages. The STAT1 is phosphorylated and translocated into the nucleus to activate transcription of its target genes including iNOS.[67–69] Therefore, in the present study, effects of **1**, **9**, and **11**, on phosphorylated STAT1 (p-STAT1) in the nuclear protein fraction were examined. As a result, the protein levels of p-STAT1 in nuclear protein fraction were reduced by **1**, **9**, and **11** in a concentration-dependent manner (Fig. 5). These findings suggest that inhibition of STAT1 activation is mainly involved in the inhibitory effects on iNOS expression by **1**, **9**, and **11**. The detailed mechanism of action including the difference in cytotoxic effects should be studied further.

3. Experimental

3.1. General

The following instruments were used to obtain spectral and physical data: specific rotations, Horiba SEPA-300 digital polarimeter (l = 5 cm); UV spectra, Shimadzu UV-1600 spectrometer; IR spectra, Shimadzu FTIR-8100 spectrometer; ^{1}H NMR spectra, JEOL JNM-ECA700 (700 MHz), JNM-ECA600 (600 MHz), and JNM-ECS400 (400 MHz) spectrometers; ^{13}C NMR spectra, JEOL JNM-ECA700 (175 MHz), JNM-ECA600 (150 MHz), and JNM-ECS400 (100 MHz) spectrometers with tetramethylsilane as an internal standard; EIMS and HREIMS, JEOL JMS-GCMATE mass spectrometer; FABMS and HRFABMS, JEOL JMS-SX 102A mass spectrometer; HPLC detector, Shimadzu SPD-10A UV–VIS detector (230 nm); HPLC column, Cosmosil 5C_{18}-MS-II and πNAP (250 × 4.6 mm i.d. and 250 × 20 mm i.d. for analytical and preparative purposes, respectively).

The following experimental conditions were used for chromatography (CC): highly porous synthetic resin, Diaion HP-20 (Mitsubishi Chemical, Tokyo, Japan); normal-phase silica gel CC, silica gel 60N (Kanto Chemical Co., Ltd., Tokyo, Japan; 63–210 mesh, spherical, neutral); reversed-phase ODS CC, Chromatorex ODS DM1020T (Fuji Silysia Chemical, Ltd., Aichi, Japan; 100–200 mesh); TLC, pre-coated TLC plates with silica gel 60F_{254} (Merck, 0.25 mm) (normal-phase) and silica gel RP-18 F_{254S} (Merck, 0.25 mm) (reversed-phase); reversed-phase HPTLC, pre-coated TLC plates with silica gel RP-18 WF_{254S} (Merck, 0.25 mm), detection was achieved by spraying with 1% $Ce(SO_4)_2$–10% aqueous H_2SO_4, followed by heating.

3.2. Plant material

The flower of *M. siamensis* was collected in Nakhonsithammarat Province, Thailand on September 2006. The plant material was identified by one of the authors (Y.P.). A voucher specimen (2006.09. Raj-04) of this plant is on file in our laboratory.

3.3. Extraction and isolation

Dried flowers of *M. siamensis* (1.8 kg) were extracted three times with MeOH under reflux for 3 h. Evaporation of the combined extracts under reduced pressure provided a MeOH extract (463.7 g, 25.66%). An aliquot (413.7 g) was partitioned into an EtOAc–H_2O (1:1, v/v) mixture to furnish an EtOAc-soluble fraction (110.34 g, 6.84%) and an aqueous phase. The aqueous phase was subjected to Diaion HP-20 CC (2.4 kg, H_2O → MeOH, twice) to give H_2O-eluted (217.70 g, 13.50%) and MeOH-eluted (68.10 g, 4.22%) fractions, respectively. An aliquot (89.45 g) of the EtOAc-soluble fraction was subjected to normal-phase silica gel CC [3.0 kg, *n*-hexane–EtOAc (10:1 → 7:1 → 5:1, v/v) → EtOAc → MeOH] to give 11 fractions [Fr. 1 (3.05 g), Fr. 2 (2.86 g), Fr. 3 (11.71 g), Fr. 4 (1.62 g), Fr. 5 (4.15 g), Fr. 6 (6.29 g), Fr. 7 (2.21 g), Fr. 8 (2.94 g), Fr. 9 (10.23 g), Fr. 10 (11.17 g), and Fr. 11 (21.35 g)]. The fraction

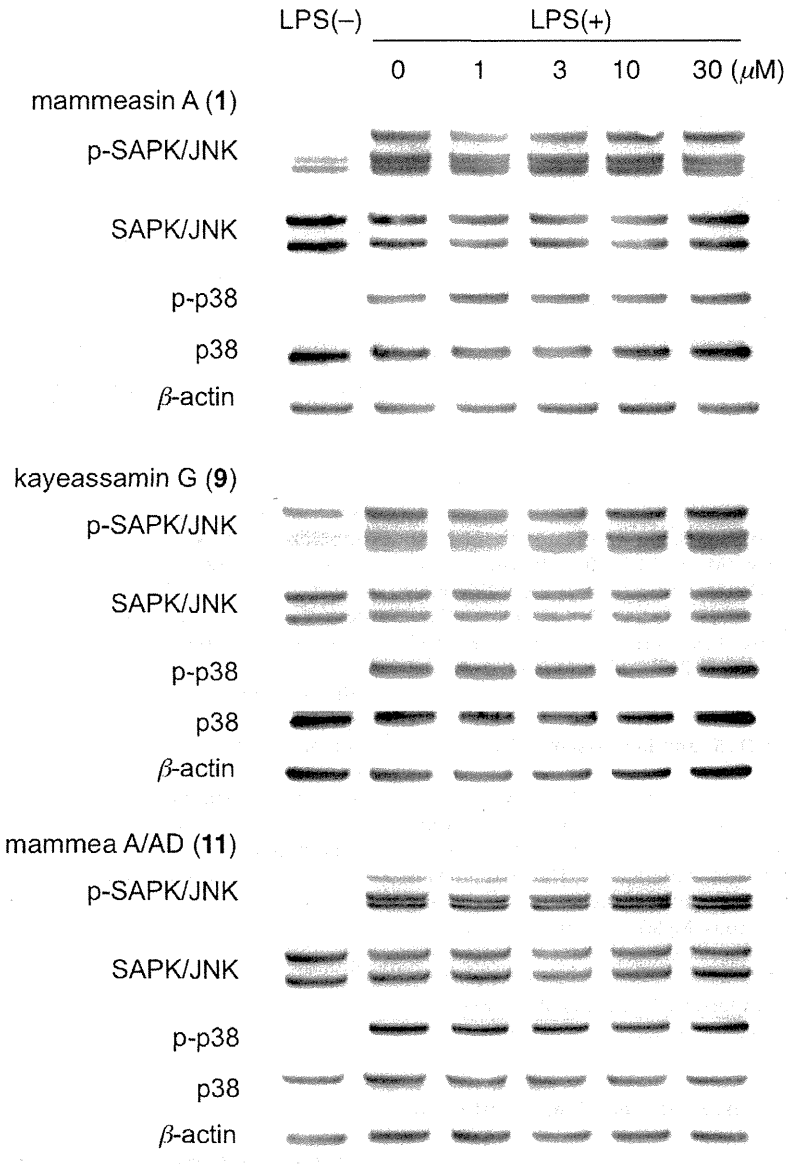

Figure 6. Effects of **1**, **9**, and **11** on SAPK/JNK, p-SPK/JNK, p-p38, and p38 protein levels.

3 (11.71 g) was subjected to reversed-phase ODS CC [340 g, MeOH–H_2O (90:10 → 95:5, v/v) → MeOH → acetone] to afford seven fractions [Fr. 3–1 (49.3 mg), Fr. 3–2 (3109.8 mg), Fr. 3–3 (4679.3 mg), Fr. 3–4 (1089.1 mg), Fr. 3–5 (1034.0 mg), Fr. 3–6 (280.8 mg), and Fr. 3–7 (85.6 mg)]. The fraction 3–4 (497.9 mg) was purified by HPLC [Cosmosil $5C_{18}$-MS-II, MeOH–1% aqueous AcOH (90:10, v/v)] to give mammea A/AB cyclo D (**12**, 27.8 mg, 0.0047%), mammea A/AC cyclo D (**13**, 46.0 mg, 0.0077%), mammea B/AB cyclo D (**14**, 9.8 mg, 0.0016%), and mammea B/AC cyclo D (**15**, 32.9 mg, 0.0055%). The fraction 3–5 (502.8 mg) was purified by HPLC [Cosmosil $5C_{18}$-MS-II, MeOH–1% aqueous AcOH (95:5, v/v)] to give surangins C (**4**, 8.2 mg, 0.0013%) and D (**5**, 24.9 mg, 0.0039%), and β-amyrin (46.0 mg, 0.0072%). The fraction 6 (6.29 g) was subjected to reversed-phase ODS CC [200 g, MeOH–H_2O (80:20 → 90:10 → 95:5, v/v) → MeOH → acetone] to afford 10 fractions [Fr. 6–1 (44.7 mg), Fr. 6–2 (157.2 mg), Fr. 6–3 (928.8 mg), Fr. 6–4 (3117.0 mg), Fr. 6–5 (128.8 mg), Fr. 6–6 (487.1 mg), Fr. 6–7 (230.8 mg), Fr. 6–8 (280.5 mg), Fr. 6–9 (102.9 mg), and Fr. 6–10 (96.5 mg)]. The fraction 6–3 (514.6 mg) was purified by HPLC [Cosmosil $5C_{18}$-MS-II, MeOH–1% aqueous AcOH (80:20, v/v)] to give mammea A/AC (**10**, 35.6 mg, 0.0049%), mammea A/AD (**11**, 15.8 mg, 0.0022%), and mammea E/BB (**16**, 140.1 mg, 0.0194%). The fraction 6–4 (536.2 mg) was purified by HPLC [Cosmosil $5C_{18}$-MS-II, MeOH–1% aqueous AcOH (90:10, v/v)] to give mammeasins A (**1**, 65.8 mg, 0.0293%) and B (**2**, 21.6 mg, 0.0096%), surangin B (**3**, 58.2 mg, 0.0259%), and **10** (112.6 mg, 0.0501%). The fraction 6–5 (128.8 mg) was purified by HPLC [Cosmosil $5C_{18}$-MS-II, MeOH–1% aqueous AcOH (90:10, v/v)] to give **2** (24.1 mg, 0.0019%) and **3** (15.1 mg, 0.0012%). The fraction 6–6 (487.1 mg) was purified by HPLC [Cosmosil $5C_{18}$-MS-II, MeOH–1% aqueous AcOH (90:10, v/v)] to give **10** (6.0 mg, 0.00050%). The fraction 9 (10.23 g) was subjected to reversed-phase ODS CC [300 g, MeOH–H_2O (80:20 → 90:10, v/v) → MeOH → acetone] to afford five fractions [Fr. 9–1 (2809.0 mg), Fr. 9–2 (5678.0 mg), Fr. 9–3 (385.9 mg), Fr. 9–4 (422.0 mg), and Fr. 9–5 (51.9 mg)]. The fraction 9–1 (544.5 mg) was purified by HPLC [Cosmosil $5C_{18}$-MS-II, MeOH–1% aqueous AcOH (85:15, v/v)] to give kayeassamins E (**7**, 28.6 mg, 0.0113%),

F (**8**, 98.7 mg, 0.0390%), and G (**9**, 43.4 mg, 0.0171%), deacetylmammea E/BC cyclo D (**17**, 18.6 mg, 0.0073%), and benzoic acid (10.9 mg, 0.0043%). The fraction 9–2 (526.2 mg) was purified by HPLC [Cosmosil $5C_{18}$-MS-II, MeOH–1% aqueous AcOH (90:10, v/v)] to give **4** (63.6 mg, 0.0525%), **5** (66.7 mg, 0.0551%), and kayeassamin A (**6**, 68.1 mg, 0.0562%). The fraction 9–3 (385.9 mg) was purified by HPLC [Cosmosil $5C_{18}$-MS-II, MeOH–1% aqueous AcOH (90:10, v/v)] to give **4** (43.1 mg, 0.0033%), **5** (54.3 mg, 0.0042%), and **6** (20.5 mg, 0.0016%).

3.3.1. Mammeasin A (1)

Pale yellow oil, $[\alpha]_D^{27}$ −29.7 (*c* 1.08, MeOH), $[\alpha]_D^{27}$ −25.4 (*c* 1.08, $CHCl_3$). EIMS (*m/z*, %): 484 (M^+, 7), 301 (100). High-resolution EIMS: Anal. Calcd for $C_{28}H_{36}O_7$ (M^+): 484.2461. Found: 484.2466. UV [MeOH, nm (log ε)]: 223 (4.62), 330 (4.65). IR (film): 3503, 1748, 1717, 1609, 1458, 1399, 1233, 1194, 1136 cm^{-1}. ^1H NMR (700 MHz, $CDCl_3$) δ: given in Table 2. ^{13}C NMR (175 MHz, $CDCl_3$) δ_C: given in Table 3.

3.3.2. Mammeasin B (2)

Pale yellow oil, $[\alpha]_D^{27}$ −19.2 (*c* 0.30, MeOH), $[\alpha]_D^{26}$ −18.4 (*c* 0.30, $CHCl_3$). EIMS (*m/z*, %): 498 (M^+, 8), 315 (100). High-resolution EIMS: Anal. Calcd for $C_{29}H_{38}O_7$ (M^+): 498.2618. Found: 498.2622. UV [MeOH, nm (log ε)]: 223 (4.48), 331 (4.58). IR (film): 3500, 1744, 1719, 1607, 1458, 1404, 1233, 1196, 1132 cm^{-1}. ^1H NMR (700 MHz, $CDCl_3$) δ: given in Table 2. ^{13}C NMR (175 MHz, $CDCl_3$) δ_C: given in Table 3.

3.4. Acetylation of surangin D (5) and kayeassamin A (6)

To a solution of **5** (4.5 mg) in pyridine (1.0 mL) was added Ac_2O (0.8 mL), and the mixture was stirred at room temperature for 24 h. The reaction mixture was poured into water and the resulting mixture was extracted with EtOAc. The extract was washed with 5% aqueous HCl, saturated aqueous $NaHCO_3$, and brine, then dried over anhydrous $MgSO_4$ and filtered. Removal of the solvent under reduced pressure gave a pale yellow oil, which was purified by HPLC [Cosmosil $5C_{18}$-MS-II, MeOH–1% aqueous AcOH (90:10, v/v)] to furnish **1** (4.3 mg, 88%). According to the similar procedure, **2** (4.2 mg, quant.) was obtained from **6** (3.6 mg).

3.5. Preparation of (*R*)-MTPA ester (5a) and (*S*)-MTPA ester (5b) from surangin D (5)

A solution of **5** (2.3 mg) in pyridine (1.0 mL) was treated with (*S*)-(+)-α-methoxy-α-(trifluoromethyl)phenylacetic chloride [(*S*)-(+)-MTPA-Cl, 7.5 μL] and the mixture was stirred at room temperature for 24 h. The reaction mixture was poured into ice-water and extracted with EtOAc. The extract was successively washed with 5% aqueous HCl, saturated aqueous $NaHCO_3$, and brine, then dried over anhydrous $MgSO_4$ and filtered. Removal of the solvent from the filtrate under reduced pressure furnished a pale yellow oil, which was purified by HPLC [Cosmosil $5C_{18}$-MS-II, MeOH–1% aqueous AcOH (90:10, v/v)] to give the (*R*)-MTPA ester derivative (**5a**, 0.9 mg, 26%). According to the similar procedure, **5b** (0.5 mg, 14%) was obtained from **5** (2.5 mg) by using (*R*)-(−)-MTPA-Cl (7.5 μL).

3.5.1. Compound 5a

^1H NMR (400 MHz, $CDCl_3$) δ: 1.03 (6H, d, *J* = 6.8 Hz, H_3-4‴, 5‴), 1.05 (3H, t, *J* = 6.8 Hz, H_3-1″), 1.61 (3H, br s, H_3-10″), 1.68 (3H, br s, H_3-9″), 1.77, 2.01 (1H each, both m, H_2-2′), 1.88 (3H, br s, H_3-5″), 3.49 (3H, s, $-OCH_3$), 5.07 (1H, br t-like, H-7″), 5.27 (1H, br dd-like, H-2″), 5.63 (1H, dd-like, H-1′), 5.83 (1H, br s, H-3) [7.45 (3H, m), 7.52 (2H, m), Ph-H].

3.5.2. Compound 5b

^1H NMR (400 MHz, $CDCl_3$) δ: 1.04 (3H, t, *J* = 6.6 Hz, H_3-1″), 1.06 (6H, d, *J* = 6.6 Hz, H_3-4‴, 5‴), 1.60 (3H, br s, H_3-10″), 1.64 (3H, br s, H_3-9″), 1.76 (3H, br s, H_3-5″), 1.76, 2.00 (1H each, both m, H_2-2′), 3.49 (3H, s, $-OCH_3$), 5.06 (1H, br t-like, H-7″), 5.27 (1H, br dd-like, H-2″), 5.64 (1H, dd-like, H-1′), 5.88 (1H, br s, H-3) [7.46 (3H, m), 7.54 (2H, m), Ph-H].

3.6. Bioassay

3.6.1. Cell culture

The murine macrophage cells (RAW264.7, ATCC No. TIB-71) were obtained from Dainippon Pharmaceutical, Osaka, Japan and cultured in Dulbecco's modified Eagle's medium (DMEM, containing 4500 mg/L glucose) supplemented with 10% fetal bovine serum (FBS), penicillin (100 U/mL), and streptomycin (100 μg/mL) (Sigma Chemical Co., St. Louis, MO, USA). The cells were incubated at 37 °C in 5% CO_2/air.

3.6.2. Effects on production of NO in LPS-stimulated macrophage RAW264.7 cells

The total amount of nitrite in a medium is used as an indicator of NO synthesis.[59] The screening test for NO production using RAW264.7 cells was described previously.[58,59] Briefly, RAW264.7 cells were cultured in DMEM, and the suspension of the cells were seeded into a 96-well microplate at 2.5×10^5 cells/100 μL/well. After 6 h, nonadherent cells were removed by washing with PBS, and the adherent cells were cultured in 100 μL of fresh medium containing the test compounds for 10 min, and then 100 μL of the medium containing LPS (from *Escherichia coli*, 055: B5, Sigma) was added to stimulate the cells for 18 h (final concentration of LPS was 10 μg/mL). The nitrite concentration was measured from the supernatant by Griess reaction. Inhibition (%) was calculated using the following formula and the IC_{50} was determined graphically ($N = 4$). Caffeic acid phenethyl ester (CAPE), an inhibitor of NF-κB activation, was used as a reference compound.[59,60].

$$\text{Inhibition } (\%) = (A - B)/(A - C) \times 100$$

A–*C*: nitrite concentration (μM);
A: LPS (+), Sample (−); *B*: LPS (+), Sample (+); *C*: LPS (−), Sample (−).

3.6.3. Determination of cytotoxic effects

Cytotoxicity was evaluated by the 3-(4,5-dimethyl-2-thiazolyl)-2,5-diphenyl-2*H*- tetrazolium bromide (MTT) colorimetric assay according to the previous reported conditions.[59] Briefly, RAW264.7 cells were cultured in DMEM, and the suspension of the cells were seeded into a 96-well microplate at 1.0×10^5 cells/200 μL/well. After 6 h, nonadherent cells were removed by washing with PBS, and the adherent cells were cultured in 100 μL of fresh medium containing the test compounds for 18 h. An aliquot of the medium (100 μL) was removed and MTT (10 μL, 5 mg/mL in PBS) solution was added. After a 2-h incubation at 37 °C, the medium was removed, and isopropanol containing 0.04 M HCl was added to dissolve the formazan produced in the cells. The optical density (OD) of the formazan solution was measured with a microplate reader at 570 nm (reference: 655 nm).

3.6.4. SDS–PAGE and Western blot analysis

RAW264.7 cells (5.0×10^6 cells/2 mL/well) were seeded into a 6-well multiplate and allowed to adhere for 6 h at 37 °C in a humidified atmosphere containing 5% CO_2. The cells were then washed with PBS, 1 mL of DMEM containing various concentrations of the

samples was added to each well, and after incubation for 10 min, 1 mL of DMEM containing LPS was added to stimulate the cells for 30 min or 12 h (final concentration of LPS, 10 μg/mL). The adhered cells were collected using a cell scraper in a lysis buffer (15 mM NaCl, 1 mM Tris, 1% Triton-X, 0.2 mM EGTA, 2.8 mM β-glycerophosphate) containing protease inhibitor cocktail (Thermo Scientific) and phosphatase inhibitor cocktail (PhosSTOP, Roche). Then, cells were disrupted three times (Microson™ ultrasonic cell disruptor, USA) for 30 s, and centrifuged at 10,000 rpm for 10 min. Protein concentrations of cell lysates were determined using the BCA™ protein assay kit. For protein sample preparation; 100 μL of supernatant was transferred to 50 μL of a dissolving agent (0.9 mM EGTA, 200 mM SDS, 2.8 mM Tris, 8% glycerol, 0.03% bromophenol blue, 6% mercaptoethanol). Then, the samples were heated in boiling water for 5 min. After cooling down, the samples were kept at −80 °C until used.[58,59]

Nuclear protein fraction was extracted 30 min after the stimulation with LPS using Nuclear and Cytoplasmic Extraction Reagent (Thermo Scientific) according to the manufacturer's instructions. The nuclear protein solution was concentrated using a Centrifugal Filter Units (Millipore Co., Ltd.) and applied for the electrophoresis.

Equivalent amounts of protein (50 μg of protein/lane for iNOS and β-actin, 25 μg of protein/lane for others) were electrophoresed in 10% SDS–polyacrylamide gels (Bio-Rad ready gel J) and transferred onto a polyvinylidene difluoride (PVDF) membranes (Bio-Rad, HC, USA). The membrane was then soaked in Tris-buffered saline containing 0.1% Tween 20 (T-TBS) with gentle shaking for 10 min, three times. For the blocking of the nonspecific sites, the membrane was soaked in Blocking One-P (for phosphorylated proteins: p-ERK1/2, p-JNK, p-p38, p-STAT1; Nacalai Tesque, Japan) or Blocking One (for others: iNOS, ERK1/2, JNK, p38, NF-κB, β-actin) by shaking for 0.5 h. The membrane was rinsed with T-TBS and incubated with specific primary antibodies: p-ERK1/2, ERK1/2, JNK1/2, p38, p-p38, NF-κB p65, STAT1, p-STAT1 (Ser 727), iNOS and β-actin (1:1000, Cell Signaling Technology). After incubation for 1 h at rt, the membrane was rinsed in T-TBS, and incubated in secondary antibodies (HRP-conjugated goat anti-mouse and anti-rabbit IgG, 1:5000) in an immunoreaction enhancer solution (Can Get Signal, Toyobo, Japan) for 1 h. Next, the membrane was shaken in T-TBS for 10 min, three times. The proteins were detected using an enhanced chemiluminescence (ECL) plus Western blotting detection system (Amersham™ GE Healthcare, Biosciences). The images of membranes were recorded using a luminescent image analyzer LAS-4000 mini (Fuji film, Japan). In our preliminary experiments, the amount of iNOS protein markedly increased 6 h after the treatment with LPS and remained higher after 24 h, and levels of p-ERK, p-JNK, p-p38, and p-STAT1 increased after 10 or 30 min and remained high for several hours (data not shown). Therefore, the effects of test compounds on iNOS protein levels were determined 12 h after the stimulation, and on other protein levels were determined 0.5 h after the stimulation.

3.7. Statistical analysis

All data are expressed as means ± SEM. The data analysis was performed with an one-way analysis of variance (1-ANOVA), followed by Dunnett's test. Probability (p) value of less than 0.05 was considered to be significant.

Acknowledgments

This work was supported by a Grant-in Aid for Scientific Research by the Japan Society for the Promotion of Science (JSPS).

References and notes

1. Poobrasert, O.; Constant, H. L.; Beecher, C. W. W.; Farnsworth, N. R.; Kinghorn, A. D.; Pezzuto, J. M.; Cordell, G. A.; Santisuk, T.; Reutrakul, V. *Phytochemistry* **1998**, *47*, 1661.
2. Mahidol, C.; Kaweetripob, W.; Prawat, H.; Ruchirawat, S. *J. Nat. Prod.* **2002**, *65*, 757.
3. Subhadhirasakul, S.; Pechpongs, P. *Songklanakarin J. Sci. Technol.* **2005**, *27*(Suppl. 2), 555.
4. Laphookhieo, S.; Maneerat, W.; Kiattansakul, R. *Can. J. Chem.* **2006**, *84*, 1546.
5. Prachyawarakorn, V.; Mahidol, C.; Ruchirawat, S. *Phytochemistry* **2006**, *67*, 924.
6. Laphookhieo, S.; Promnart, P.; Syers, J. K.; Kanjana-Opas, A.; Ponglimanont, C.; Karalai, C. *J. Braz. Chem. Soc.* **2007**, *18*, 1077.
7. Ngo, N. T. N.; Nguyen, V. T.; Vo, H. V.; Vang, O.; Duus, F.; Ho, T.-D. H.; Pham, H. D.; Nguyen, L.-H. D. *Chem. Pharm. Bull.* **2010**, *58*, 1487.
8. Kaweetripob, W.; Mahidol, C.; Prawat, H.; Ruchirawat, S. *Pharm. Biol.* **2000**, *38*(Suppl.), 55.
9. Mahidol, C.; Prawat, H.; Kaweetripob, W.; Ruchirawat, S. *Nat. Prod. Commun.* **2007**, *2*, 557.
10. Morikawa, T.; Xu, F.; Matsuda, H.; Yoshikawa, M. *Chem. Pharm. Bull.* **2006**, *54*, 1530.
11. Yoshikawa, M.; Xu, F.; Morikawa, T.; Pongpiriyadacha, Y.; Nakamura, S.; Asao, Y.; Kumahara, A.; Matsuda, H. *Chem. Pharm. Bull.* **2007**, *55*, 308.
12. Matsuda, H.; Ninomiya, K.; Morikawa, T.; Yasuda, D.; Yamaguchi, I.; Yoshikawa, M. *Bioorg. Med. Chem. Lett.* **2008**, *18*, 2038.
13. Yoshikawa, M.; Morikawa, T.; Funakoshi, K.; Ochi, M.; Pongpiriyadacha, Y.; Matsuda, H. *Heterocycles* **2008**, *75*, 1639.
14. Morikawa, T.; Funakoshi, K.; Ninomiya, K.; Yasuda, D.; Miyagawa, K.; Matsuda, H.; Yoshikawa, M. *Chem. Pharm. Bull.* **2008**, *56*, 956.
15. Morikawa, T.; Xie, Y.; Asao, Y.; Okamoto, M.; Yamashita, C.; Muraoka, O.; Matsuda, H.; Pongpiriyadacha, Y.; Yuan, D.; Yoshikawa, M. *Phytochemistry* **2009**, *70*, 1166.
16. Asao, Y.; Morikawa, T.; Xie, Y.; Okamoto, M.; Hamao, M.; Matsuda, H.; Muraoka, O.; Yuan, D.; Yoshikawa, M. *Chem. Pharm. Bull.* **2009**, *57*, 198.
17. Matsuda, H.; Ninomiya, K.; Morikawa, T.; Yasuda, D.; Yamaguchi, I.; Yoshikawa, M. *Bioorg. Med. Chem.* **2009**, *17*, 7313.
18. Morikawa, T.; Yamaguchi, I.; Matsuda, H.; Yoshikawa, M. *Chem. Pharm. Bull.* **2009**, *57*, 1292.
19. Muraoka, O.; Morikawa, T.; Miyake, S.; Akaki, J.; Ninomiya, K.; Yoshikawa, M. J. *Pharm. Biomed. Anal.* **2010**, *52*, 770.
20. Morikawa, T. *Yakugaku Zasshi* **2010**, *130*, 785.
21. Morikawa, T.; Xie, Y.; Ninomiya, K.; Okamoto, M.; Muraoka, O.; Yuan, D.; Yoshikawa, M.; Hayakawa, T. *Chem. Pharm. Bull.* **2010**, *58*, 1276.
22. Muraoka, O.; Morikawa, T.; Miyake, S.; Akaki, J.; Ninomiya, K.; Pongpiriyadacha, Y.; Yoshikawa, M. *J. Nat. Med.* **2011**, *65*, 142.
23. Xie, W.; Tanabe, G.; Akaki, J.; Morikawa, T.; Ninomiya, K.; Minematsu, T.; Yoshikawa, M.; Wu, X.; Muraoka, O. *Bioorg. Med. Chem.* **2011**, *19*, 2015.
24. Chaipech, S.; Morikawa, T.; Ninomiya, K.; Yoshikawa, M.; Pongpiriyadacha, Y.; Hayakawa, T.; Muraoka, O. *Chem. Pharm. Bull.* **2012**, *60*, 62.
25. Morikawa, T.; Chaipech, S.; Matsuda, H.; Hamao, M.; Umeda, Y.; Sato, H.; Tamura, H.; Kon'i, H.; Ninomiya, K.; Yoshikawa, M.; Pongpiriyadacha, Y.; Hayakawa, T.; Muraoka, O. *Bioorg. Med. Chem.* **2012**, *20*, 832.
26. Chaipech, S.; Morikawa, T.; Ninomiya, K.; Yoshikawa, M.; Pongpiriyadacha, Y.; Hayakawa, T.; Muraoka, O. J. *Nat. Med.* **2012**, *66*, 486.
27. Morikawa, T.; Chaipech, S.; Matsuda, H.; Hamao, M.; Umeda, Y.; Sato, H.; Tamura, H.; Ninomiya, K.; Yoshikawa, M.; Pongpiriyadacha, Y.; Hayakawa, T.; Muraoka, O. J. *Nat. Med.* **2012**, *66*, 516.
28. Joshi, B. S.; Kamat, V. N.; Govindachari, T. R.; Ganguly, A. K. *Tetrahedron* **1969**, *25*, 1453.
29. Crombie, L.; Games, D. E.; Haskins, N. J.; Read, G. F. *Tetrahedron Lett.* **1970**, *3*, 251.
30. Deng, Y.; Nicholson, R. A. *Planta Med.* **2005**, *71*, 364.
31. Verotta, L.; Lovaglio, E.; Vidari, G.; Finzi, P. V.; Neri, M. G.; Raimondi, A.; Parapini, S.; Taramelli, D.; Riva, A.; Bombardelli, E. *Phytochemistry* **2004**, *65*, 2867.
32. Yagi, N.; Ohkubo, K.; Okuno, Y.; Oda, Y.; Miyazawa, M. *J. Oleo Sci.* **2006**, *55*, 173.
33. Win, N. N.; Awale, S.; Esumi, H.; Tezuka, Y.; Kadota, S. *Bioorg. Med. Chem. Lett.* **2008**, *18*, 4688.
34. Win, N. N.; Awale, S.; Esumi, H.; Tezuka, Y.; Kadota, S. *Bioorg. Med. Chem.* **2008**, *16*, 8653.
35. Thebtaranonth, C.; Imraporn, S.; Padungkul, N. *Phytochemistry* **1981**, *20*, 2305.
36. Morel, C.; Guilet, D.; Oger, J.-M.; Séraphin, D.; Sévenet, T.; Wiart, C.; Hadi, A. H. A.; Richomme, P.; Bruneton, J. *Phytochemistry* **1999**, *50*, 1243.
37. Crombie, L.; Jones, R. C. F.; Palmer, C. J. *J. Chem. Soc., Perkin Trans. 1* **1987**, 317.
38. Cruz, F. G.; da Silva-Neto, J. T.; Guedes, M. L. S. *J. Braz. Chem. Soc.* **2001**, *12*, 117.
39. Yang, H.; Protiva, P.; Gil, R. R.; Jiang, B.; Baggett, S.; Basile, M. J.; Reynertson, K. A.; Weinstein, I. B.; Kennelly, E. J. *Planta Med.* **2005**, *71*, 852.
40. β-Amyrin and benzoic acid were identified by comparison of their physical data with those of commercially obtained samples.
41. The ^{1}H and ^{13}C NMR spectra of **1** and **2** were assigned with the aid of distortionless enhancement by polarization transfer (DEPT), 1H–1H correlation spectroscopy (^{1}H–^{1}H COSY), heteronuclear multiple quantum coherence (HMQC), and heteronuclear multiple bond correlation spectroscopy (HMBC) experiments.

42. Ohtani, I.; Kusumi, T.; Kashman, Y.; Kakisawa, H. J. *Am. Chem. Soc.* **1991**, *113*, 4092.
43. Kontush, A.; Chapman, M. J. *Pharmcol. Rev.* **2006**, *58*, 342.
44. Hansson, G. K. *New Eng. J. Med.* **2005**, *352*, 1685.
45. MacMicking, J.; Xie, Q. W.; Nathan, C. *Ann. Rev. Immunol.* **1997**, *15*, 323.
46. Rao, Y. K.; Fang, S. H.; Tzeng, Y. M. *J. Ethnopharmacol.* **2005**, *100*, 249.
47. Qu, D. M.; Zheng, Y. G. *Pathophysiol. Clin. Med.* **1997**, *17*, 270.
48. Luo, Y.; Wu, K.; Sun, A.; Pan, B.; Zhang, X.; Fan, D. *Chin. J. Digest. Dis.* **2001**, *2*, 120.
49. Bogdan, C. *Nat. Immunol.* **2001**, *2*, 907.
50. Kumar, A. P.; Ryan, C.; Cordy, V.; Reynolds, W. F. *Nitric Oxide* **2005**, *13*, 2.
51. Zang, M. W.; Liu, J. S. *Pathophysiol. Clin. Med.* **1998**, *18*, 37.
52. Matsuda, H.; Ando, S.; Kato, T.; Morikawa, T.; Yoshikawa, M. *Bioorg. Med. Chem.* **2006**, *14*, 138.
53. Yoshikawa, M.; Nishida, N.; Ninomiya, K.; Ohgushi, T.; Kubo, M.; Morikawa, T.; Matsuda, H. *Bioorg. Med. Chem.* **2006**, *14*, 456.
54. Morikawa, T.; Abdel-Halim, O. B.; Matsuda, H.; Ando, S.; Muraoka, O.; Yoshikawa, M. *Tetrahedron* **2006**, *62*, 6435.
55. Morikawa, T. *J. Nat. Med.* **2007**, *61*, 112.
56. Yoshikawa, M.; Morikawa, T.; Oominami, H.; Matsuda, H. *Chem. Pharm. Bull.* **2009**, *57*, 957.
57. Morikawa, T.; Oominami, H.; Matsuda, H.; Yoshikawa, M. *J. Nat. Med.* **2011**, *65*, 129.
58. Sae-Wong, C.; Matsuda, H.; Tewtrakul, S.; Tansakul, P.; Nakamura, S.; Nomura, Y.; Yoshikawa, M. *J. Ethnopharmacol.* **2011**, *136*, 488.
59. Hegazy, M. E.; Matsuda, H.; Nakamura, S.; Yabe, M.; Matsumoto, T.; Yoshikawa, M. *Chem. Pharm. Bull.* **2012**, *60*, 363.
60. Natarajan, K.; Singh, S.; Burke, T. R., Jr.; Grunber-ger, D.; Aggarwal, B. B. *Proc. Natl. Acad. Sci. U.S.A.* **1996**, *93*, 9090.
61. Kieran, M. W.; Zon, L. I. *Curr. Opin. Hematol.* **1996**, *3*, 27.
62. Kurosawa, M.; Numazawa, S.; Tani, Y.; Yoshida, T. *Am. J. Physiol. Cell Physiol.* **2000**, *278*, 500.
63. Moon, D. O.; Park, S. Y.; Lee, K. J.; Heo, M. S.; Kim, K. C.; Kim, M. O.; Lee, J. D.; Choi, Y. H.; Kim, G. Y. *Int. Immunopharmacol.* **2007**, *7*, 1092.
64. Park, H. J.; Lee, H. J.; Choi, M. S.; Son, D. J.; Song, H. S.; Song, M. J.; Lee, J. M.; Han, S. B.; Kim, Y.; Hong, J. T. *J. Inflamm. (Lond.)* **2008**, *5*, 7.
65. Lin, H. T.; Shen, S. C.; Lin, C. W.; Wu, M. S.; Chen, Y. C. *Chem. Biol. Interact.* **2009**, *180*, 202.
66. Hwang, J. M.; Yu, J. Y.; Jang, Y. O.; Kim, B. T.; Hwang, K. J.; Jeon, Y. M.; Lee, J. C. *Int. Immunopharmacol.* **2010**, *10*, 526.
67. Kawai, T.; Takeuchi, O.; Fujita, T.; Inoue, J.; Muhlradt, P. F.; Sato, S.; Hoshino, K.; Akira, S. *J. Immunol.* **2001**, *167*, 5887.
68. Ando, S.; Matsuda, H.; Morikawa, T.; Yoshikawa, M. *Bioorg. Med. Chem.* **2005**, *13*, 3289.
69. Shen, T.; Park, Y. C.; Kim, S. H.; Lee, J.; Cho, J. Y. *Biol. Pharm. Bull.* **2010**, *33*, 1159.

Journal of Chromatography B, 928 (2013) 16–21

Contents lists available at SciVerse ScienceDirect

Journal of Chromatography B

journal homepage: www.elsevier.com/locate/chromb

Free glycans derived from glycoproteins present in human sera

Kinya Iwatsuka[a], Sakie Watanabe[a], Mitsuhiro Kinoshita[a], Kazuya Kamisue[a], Keita Yamada[a], Takao Hayakawa[b], Tadashi Suzuki[c], Kazuaki Kakehi[a,*]

[a] Faculty of Pharmaceutical Sciences, Kinki University, 3-4-1 Kowakae, Higashi-Osaka 577-8502, Japan
[b] Pharmaceutical Research and Technology Institute, Kinki University, Kowakae 3-4-1, Higashi-osaka 577-8502, Japan
[c] Glycometabolome Laboratory, Frontier Research System, RIKEN (The Institute for Physical and Chemical Research), 2-1 Hirosawa, Wako, Saitama 351-0198, Japan

ARTICLE INFO

Article history:
Received 15 December 2012
Accepted 12 March 2013
Available online 21 March 2013

Keywords:
Free glycans
Serum
Transferrin
HPLC
ESI-TOF-MS

ABSTRACT

During the course of studies on the analysis of O-glycans in biological samples, we found that significant amount of free glycans are present in normal human serum samples. The most abundant free glycan was disialo-biantennary glycan typically observed in transferrin which is one of the abundant glycoproteins found in sera. Minor glycans were also considered to be mainly due to transferrin, but some glycans were derived from mucin-type O-glycans, although the amount was quite minute. However, high mannose-type glycans could not be detected at all. Although there have been many reports on the presence of intracellular "free" N-glycans (mainly derived from high mannose-type glycans) generated either from lipid-linked oligosaccharides or from misfolded glycoproteins through endoplasmic-reticulum associated protein degradation pathway, there is little information on the presence of free glycans in extracellular matrix and biological fluids such as serum. This report is the first one which demonstrates the presence of free glycans due to glycoproteins in sera.

1. Introduction

There have been many reports on the presence of free glycans in cytosols, and the formation of such free glycans is an important clue for the understanding the selection of properly synthesized glycoproteins. Such free glycans found in cytosols are exclusively high mannose-type glycans having one N-acetylglucosamine (GlcNAc) residue at the reducing termini [1,2], and are formed in the cytosol by a cellular system called ERAD (endoplasmic reticulum-associated degradation) [3]. Such intracellular "free" N-glycans are generated either from lipid-linked oligosaccharides or from misfolded glycoproteins [4–7]. In both cases, occurrence of high mannose-type free glycans, which have one GlcNAc residue at their reducing ends, has been well-documented.

Little is known with regard to the accumulation of more processed, complex-type free glycans in the cytosol of mammalian cells. In our previous report on the comprehensive analysis of N-glycans in cancer cells [8], we found that significantly large amount of unusual, complex-type free N-glycans were accumulated in stomach cancer-derived cell lines, MKN7 and MKN45. It should be noticed that all the free glycans found in these cells were cleaved between the GlcNAcβ1–4GlcNAc (i.e. chitobiose) bond and a single GlcNAc residue was present at the reducing end. In addition, most of the accumulated glycans have N-acetylneuraminic acid (NeuAc) residues at the non-reducing termini. And we showed that loss of the activity of cytosolic neuraminidase, Neu2, was responsible for the accumulation of such unusual free glycans [9].

In contrast, there is little information on the presence of free glycans in extracellular matrixes and biological fluids such as sera probably due to insufficient and poor ability to analyze minute amount of glycans. We have been developing sensitive methods for comprehensive analyses of N- and O-glycans in biological samples, especially cancer cells, tissues and serum samples [5,10–13]. During the course of studies on the analysis of O-glycans in biological samples, we found that significant amount of free glycans are present in human serum samples. This is unexpected and interesting, although it is well known that patients suffering from genetic lysosomal disorders of complex carbohydrate metabolism excrete a considerable amount of unusual oligosaccharides in urine [14–17].

Inoue et al. reported that free glycans were present in the unfertilized eggs of a fresh water trout, *Plecogiossus altivelis* [18]. The isolated glycans consist of desialylated biantennary glycans with β-Man-GlcNAc structure at their reducing termini. However, a small portion of the glycans having chitobiose (GlcNAcβ1-4-GlcNAc) structure at the reducing ends were also present. It is still not clear why and how such large amount of free glycans are accumulated in unfertilized eggs. Another important report on the presence of free glycans is the expression of free glycans in human seminal

* Corresponding author. Tel.: +80 6 6721 2332; fax: +80 6 6721 2353.
E-mail address: k_kakehi@phar.kindai.ac.jp (K. Kakehi).

1570-0232/$ – see front matter © 2013 Elsevier B.V. All rights reserved.
http://dx.doi.org/10.1016/j.jchromb.2013.03.010

plasma [19], and the structural characteristics are similar to those in human milk. But their variations are simpler than those of human milk oligosaccharides.

According to the reference search works on the presence of free glycans in sera, the present work demonstrating the presence of free glycans in sera is the first one, and will lead to a new research project on finding glycan-based disease biomarkers.

2. Materials and methods

2.1. Materials

Sephadex LH-20 and Asahi Shodex NH2P-50 4E column were obtained from GE Healthcare UK Ltd. (Buckinghamshire, UK) and Showa Denko (Minato-ku, Tokyo, Japan), respectively. Sodium cyanoborohydride and 2-aminobenzoic acid (2AA) were from Tokyo Kasei Kogyo (Chuo-Ku, Tokyo, Japan). TOYOPAK ODS-S for solid phase extraction was from Tosoh (Minato-ku, Tokyo, Japan). VIVASPIN 500 (3000 molecular weight cut off) for ultrafiltration was from Sigma–Aldrich Japan (Shinagawa-ku, Tokyo, Japan). All other reagents were of the highest grade commercially available. All aqueous solutions were prepared using water purified with a Milli-Q purification system (Millipore, Bedford, MA, USA).

2.2. Serum samples

Serum samples from healthy volunteers were obtained under the permission of the Ethics Committee of Kinki University School of Pharmacy, and used in accordance with the tenets of the Declaration of Helsinki.

2.3. Sample preparation

2.3.1. Ultrafiltration and solid-phase extraction of the serum sample

Because the serum sample contains a large amount of low-molecular-weight materials such as monosaccharides (typically glucose) and inorganic salts, and hydrophobic compounds, these materials should be removed prior to the analysis.

A serum sample (25 μL) was centrifuged at 15,000 × *g* using an ultramembrane filter (3000 molecular weight cut off) to remove the low-molecular weight materials, and concentrated to the one fourth volume. Water (150 μL) was added to the concentrate on the membrane, and centrifuged at 15,000 × *g* again. The procedures were repeated three times. The concentrated serum sample on the membrane was transferred to a new tube, and the membrane was washed with water (150 μL) and combined with the concentrated solution. The mixture was then passed through an ODS cartridge (90 mg) which was previously washed with methanol (0.8 mL 3×) and water (0.8 mL 3×). The clean-up procedures were performed according to the method recommended by the manufacturer.

2.3.2. Total N-glycans in a serum sample

A serum sample (150 μL) was centrifuged at 15,000 × *g* using an ultramembrane filter (3000 molecular weight cut off) to remove the low-molecular weight materials, and concentrated to dryness. The dried sample was suspended in water (200 μL) and was mixed with 10% SDS (24 μL) and 2-mercaptoethanol (2.4 μL). The mixture was kept in the boiling water bath for 5 min. After cooling, 10% NP40 (nonylphenol poly(ethylene glycol ether)$_n$) solution (24 μL) and 1 M sodium phosphate buffer (pH 7.5, 29 μL) were added. After addition of N-glycoamidase F (2 units), the mixture was kept at 37 °C overnight. After cooling, ethanol (695 μL) was added and the mixture was centrifuged at 15,000 × *g* for 10 min. The supernatant was collected and evaporated to dryness under reduced pressure.

2.3.3. Releasing reaction of O-glycans in mucin-type glycoproteins in serum samples

Releasing reaction of O-glycans from mucin-type glycoproteins present in serum samples was performed using the automated glycan releasing system according to the method reported previously [10].

2.3.4. Fluorescent labeling of glycans with 2AA

The sample of glycan mixture was dissolved in water (20 μL) and 2AA solution (100 μL) which was freshly prepared by dissolution of 2AA (15 mg) and sodium cyanoborohydride (15 mg) in methanol (500 μL) containing 4% sodium acetate and 2% boric acid. The mixture was kept at 80 °C for 1 h, and water (20 μL) and 50% (v/v) methanol (200 μL) were added to the mixture after cooling, and centrifuged at 15,000 × *g* for 10 min. The supernatant solution was applied to a column of Sephadex LH-20 (1.0 cm i.d., 30 cm length), which was previously equilibrated with 50% methanol. The earlier eluted fluorescent fractions were pooled and evaporated to dryness under reduced pressure. The residue was further purified by solid phase extraction as described above (Section 2.3.1), and evaporated to dryness.

2.3.5. Digestion of the glycan mixture with neuraminidase

Neuraminidase (1 munit, 2 μL) was added to the mixture of 2AA-labeled glycans in 20 mM acetate buffer (pH 5.0, 20 μL), and the mixture was incubated at 37 °C overnight. After keeping the mixture in the boiling water bath for 10 min followed by centrifugation, the supernatant solution was used for MS analysis.

2.4. HPLC analysis of 2AA-labeled free glycans and N-glycans in serum samples

Analysis of the 2AA-labeled glycans was performed with two Shimadzu LC-10ADvp pumps, a Jasco FP-920 fluorescence detector equipped with a polymer-based Asahi Shodex NH2P-50 4E column (4.6 mm i.d. × 250 mm). Linear gradient method was employed by 2% acetic acid in acetonitrile (solvent A) and 5% acetic acid in water containing 3% triethylamine (solvent B). The column was initially equilibrated and eluted with 30% solvent B for 2 min. Then, solvent B was increased to 95% over 80 min, and kept at this composition for further 20 min. The column effluent was monitored by a fluorescence detector set at an excitation wavelength of 350 nm and 425 nm for emission.

2.5. Liquid chromatography–electrospray ionization ion-trap time-of-flight mass spectrometry (LC–ESI-IT-TOF MS)

Negative electrospray ionization (ESI)-MS analyses were conducted with an LC–IT-TOF MS instrument (Shimadzu) connected with an HPLC system (LC-20AD pump and CBM-20A system controller; Shimadzu). The 2AA-labeled glycans were analyzed by infusion method. Isocratic elution was carried out at a flow rate of 0.2 mL/min with 50% (v/v) acetonitrile in water. The MS apparatus was operated at a probe voltage of 1.75 kV, CDL temperature of 180 °C, nebulizer gas flow of 1.5 L/min, ion accumulation time of 30 ms. MS range was from *m/z* 200 to 2000. CID parameters were as follows: energy, 50%; collision gas, 50%. MS data were processed with LCMS solution ver. 3.6 software (Shimadzu).

3. Results and discussion

3.1. Free glycans in serum samples

Fig. 1a shows the results on the analysis of O-glycans in a serum sample. In this analysis, O-glycans were previously

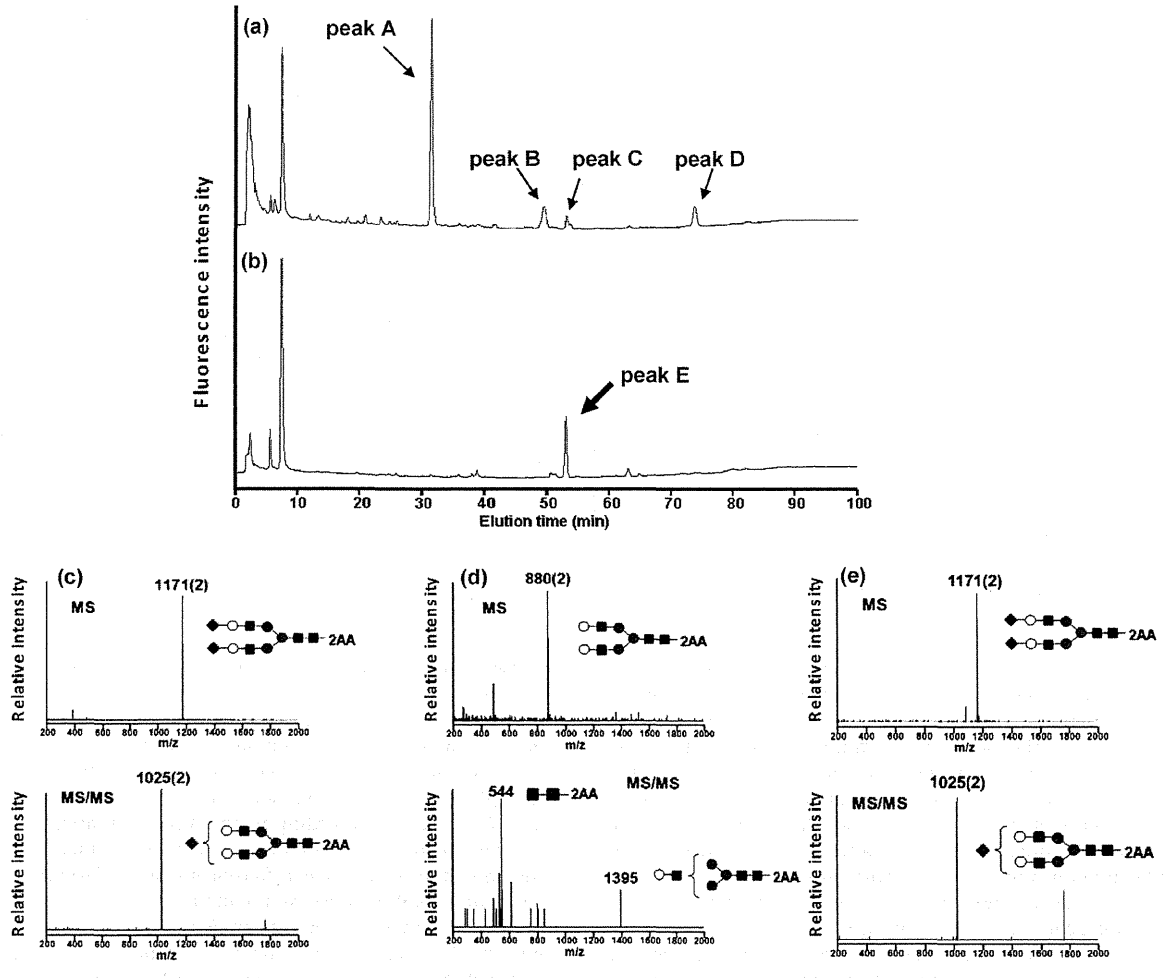

Fig. 1. HPLC Analysis of (a) mucin-type glycans from human serum released from the glycoproteins. (b) Intact serum sample after easy removal of low molecular weight materials. MS and MS/MS data of (c) peak C and (d) the product after neuraminidase digestion of peak C. (e) MS and MS/MS data of peak E. HPLC conditions: column, Asahi Shodex NH2P-50 4E(4.6 mm × 250 mm). Eluent solvent A, 2% acetic acid in acetonitrile, solvent B, 5% acetic acid, 3% triethylamine in water. Gradient condition: a linear gradient (30–95% solvent B) from 2 to 82 min, maintained for 20 min. Symbols: squares, N-acetylglucosamine; gray circles, mannose; white circles, galactose; diamonds, N-acetylneuraminic acid.

chemically released from the glycoproteins in a serum sample by an automatic manner developed by the authors [10–13], and analyzed by HPLC after labeling with a fluorescent reagent, 2AA. Four peaks (**A**–**D**) were detected at 30 (**A**), 46 (**B**), 53 (**C**) and 70 min (**D**), respectively. Peaks **A**, **B** and **D** were due to mucin-type O-glycans, and identified as sialyl T (NeuAcα2-3Galβ1-3GalNAc-2AA), degradation product (NeuAcα2–3 Gal) and disialyl T(NeuAcα2-3Galβ1-3[NeuACα2-6]GalNAc-2AA), respectively. A distinct peak (peak **C**) other than those of mucin-derived glycans was observed at 53 min. The MS and MS/MS spectra of the peak **C** are shown in Fig. 1c. The molecular ion of the peak was observed at *m/z* 1171 as a doubly charged ion, which was confirmed as disialo-biantennary glycan. And the ion due to monosialo biantennary glycan was observed in MS/MS spectra. The peak at 53 min was collected, and digested with neuraminidase. MS of the obtained asialoglycan showed the molecular ion at *m/z* 880 as a doubly charged ion (Fig. 1d). MS/MS spectra showed an ion due to chitobiosyl-2AA at *m/z* 544. These data clearly mean that peak **C** is due to disialobiantennary glycan. As indicated previously, the automatic apparatus employed for releasing O-glycans does not cleave Asn-GlcNAc linkage, and free N-glycans are not released from the protein core containing Asn-type glycoproteins [10]. This means that glycan (due to peak **C**) was endogenously present in serum samples.

To demonstrate if the glycans are due to free glycans in sera, the glycans in sera were directly analyzed after labeling with 2AA. After removing the small-molecular weight materials including glucose and inorganic salts in sera by ultrafiltration and also removing hydrophobic materials using an ODS-cartridge, the eluate (equivalent to 2 μL of sera) was analyzed by HPLC after labeling with 2-AA (Fig. 1b). A big peak (peak **E**) was observed at 53 min, which showed the same elution time with that of peak **C** observed in Fig. 1a. In addition, the peak showed the same MS and MS/MS profiles with those of peak **C** (Fig. 1e). In addition, the data also showed well matched results with those of biantennary glycan obtained from transferrin (data not shown). These results indicate that the peak at 53 min was clearly due to the glycan present in sera in free form. It should be noticed that some minor peaks were also observed from 25 min to 65 min.

3.2. Detailed analysis of free glycans in a serum sample

As described above, we found that free glycans are present in human serum samples. Fig. 2a shows the results on the detailed

Table 1
Summary of free glycans in human serum. (A) before neuraminidase digestion. (B) after neuraminidase digestion.

Peak no.	*m/z*	Monosaccharides composition	Content of free oligosaccharide (p mol/mL serum)
1	(A) 872 (2)	$Hex_4dHex_1HexNAc_4$-2AA	175
	(B) 872 (2)	$Hex_4dHex_1HexNAc_4$-2AA	
2	(A) 953 (2)	$Hex_5dHex_1HexNAc_4$-2AA	256
	(B) 953 (2)	$Hex_5dHex_1HexNAc_4$-2AA	
3, 4	(A) 794 (1)	$NeuAc_1Hex_1HexNAc_1$-2AA	264 (peak 3)
	(B) 503 (1)	$Hex_1HexNAc_1$-2AA	224 (peak 4)
5	(A) 1099 (2)	$NeuAc_1Hex_5dHex_1HexNAc_4$-2AA	235
	(B) 953 (2)	$Hex_5dHex_1HexNAc_4$-2AA	
6	(A) 1025 (2)	$NeuAc_1Hex_5HexNAc_4$-2AA	844
	(B) 880 (2)	$Hex_5HexNAc_4$-2AA	
7	(A) 1171 (2)	$NeuAc_2Hex_5HexNAc_4$-2AA	572
	(B) 880 (2)	$Hex_5HexNAc_4$-2AA	
8	(A) 1244 (2)	$NeuAc_2Hex_5dHex_1HexNAc_4$-2AA	642
	(B) 953 (2)	$Hex_5dHex_1HexNAc_4$-2AA	
9	(A) 1171 (2)	$NeuAc_2Hex_5HexNAc_4$-2AA	7620
	(B) 880 (2)	$Hex_5HexNAc_4$-2AA	
10	(A) 1070 (2)	$NeuAc_2Hex_5HexNAc_3$-2AA	235
	(B) 778 (2)	$Hex_5HexNAc_3$-2AA	
11-①	(A) 1048 (3)	$NeuAc_3Hex_6dHex_1HexNAc_5$-2AA	1206
	(B) 1136 (2)	$Hex_6dHex_1HexNAc_5$-2AA	(Total contents
11-②	(A) 999 (3)	$NeuAc_3Hex_6HexNAc_5$-2AA	for 11-① and 11-②)
	(B) 1062 (2)	$Hex_6HexNAc_5$-2AA	

dHex, deoxyhexose; Hex, hexose; HexNAc, N-acetyl hexose; NeuAc, N-acetylneuraminic acid.

profile of free glycans present in a serum sample (equivalent to 100 μL serum as the injected volume). Each peak was collected and their structures were confirmed by MS technique (Fig. 3 and Table 1). Most of the peaks are commonly found in transferrin and other commercially available samples, and their structures are easily confirmed. Disialylated biantennary glycan showing the molecular ion at *m/z* 1171 (peak **9**) as the doubly charged ion was the most abundant glycan as already shown in Fig. 1. The amount was determined to be 7620 pmol/mL of serum as calculated from the fluorescent intensity based on 2-AA residue. Structures of the minor peaks were also determined by MS techniques and comparison of the elution times with those reported previously [9]. At the earlier elution times (ca. 25 min), neutral mono- and di-galactosylated biantennary glycans (**1** and **2**) were observed. Mono-sialylated biantennary glycans with or without a fucose residue were observed at ca. 39 min (**5** and **6**). In addition, trisialo-triantennary glycans with or without a fucose residue were also observed at 63 min (**11**). Interestingly, we found a glycan having a structure of NeuAc-Gal-GalNAc-2AA which is probably due to mucin-type glycoproteins, although the amount of these glycans were only ca. 250 pmol/mL of serum (**3** and **4**). These peaks (**3** and **4**) were also assigned by comparison of the elution times with

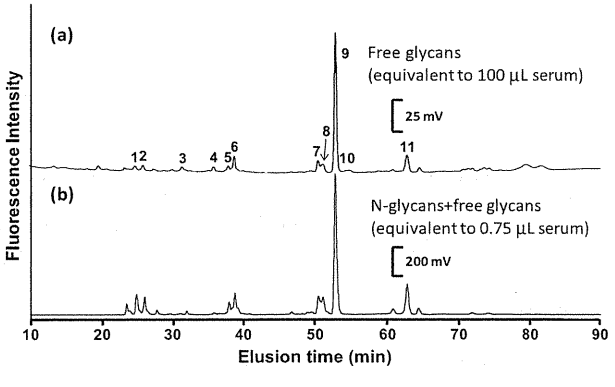

Fig. 2. HPLC analysis of (a) free glycans, and (b) total N-glycans in a human serum sample as examined after digestion with N-glycoamidase F. Analytical conditions are the same as those in Fig. 1.

those reported previously [10]. A characteristic glycan (**10**), disialo-biantennary glycan having one GlcNAc residue at the reducing end was also present in sera. We previously reported that this glycan was characteristically accumulated in cytosols of stomach tumor cells. The presence of this glycan may indicate that this characteristic glycan is leaked from some organs, although further studies are required [9]. According to the MS observations, peak **7** was assigned as disialo biantennary glycan by MS measurement. This indicates that peak **7** has different linkages of NeuAc to Gal with those of peak **9**. Because NeuAc mainly binds to Gal through α2-6 linkage in human [20], the glycan (**9**) is a typical disialo biantennary glycan which has NeuAcα2-6 linkages. And peak **7** is probably due to disialoglycan which has NeuAcα2-3 linkages. We also analyzed total N-glycans in a serum sample in order to consider the origin of free glycans in serum in detail. Fig. 2b shows the results on the profile of total N-glycans present in a serum sample (equivalent to 0.75 μL serum as the injected volume). As shown in Fig. 2b, the results are quite similar to those in Fig. 2a. It should be emphasized that high mannose-type glycans were not detected at all. This also indicates that these glycans are not due to cells from some organs but from sera, because high mannose-type glycans are major ones found in cytosol fractions through endoplasmic-reticulum associated protein degradation pathway [3].

Sturiale et al. studied glycosylation of transferrin in galactosemia patients in order to figure out hypoglycosylation with increased fucosylation and branching [21]. In the manuscript, they showed N-glycan profiles in a human serum sample (healthy volunteer) examined by MS technique after releasing N-glycans with N-glycoamidase F. The data showed quite similar profiles with those observed in the present study. Namely, Sturiale et al. reported that the ratios of triantennary glycan ($(Fuc)Gal_3GlcNAc_5Man_3NeuAc_3$), monosialo-biantennary glycan ($Gal_2GlcNAc_4Man_3NeuAc$) and disialo-fucosylated biantennary glycan ($FucGal_2GlcNAc_4Man_3NeuAc_2$) to the main glycan ($Gal_2GlcNAc_4Man_3NeuAc_2$) were 13.5, 9.4 and 6.5%, respectively. In the present study, the ratios of these glycans to the major glycan (**9**) were 15.8, 11.1 and 8.4%, respectively. These data clearly indicate that these glycans are possibly derived from serum glycoproteins containing transferrin during its circulation in bodies.

Free glycans found in the cytosol have only a single GlcNAc at their reducing termini [2], and this is due to the action of

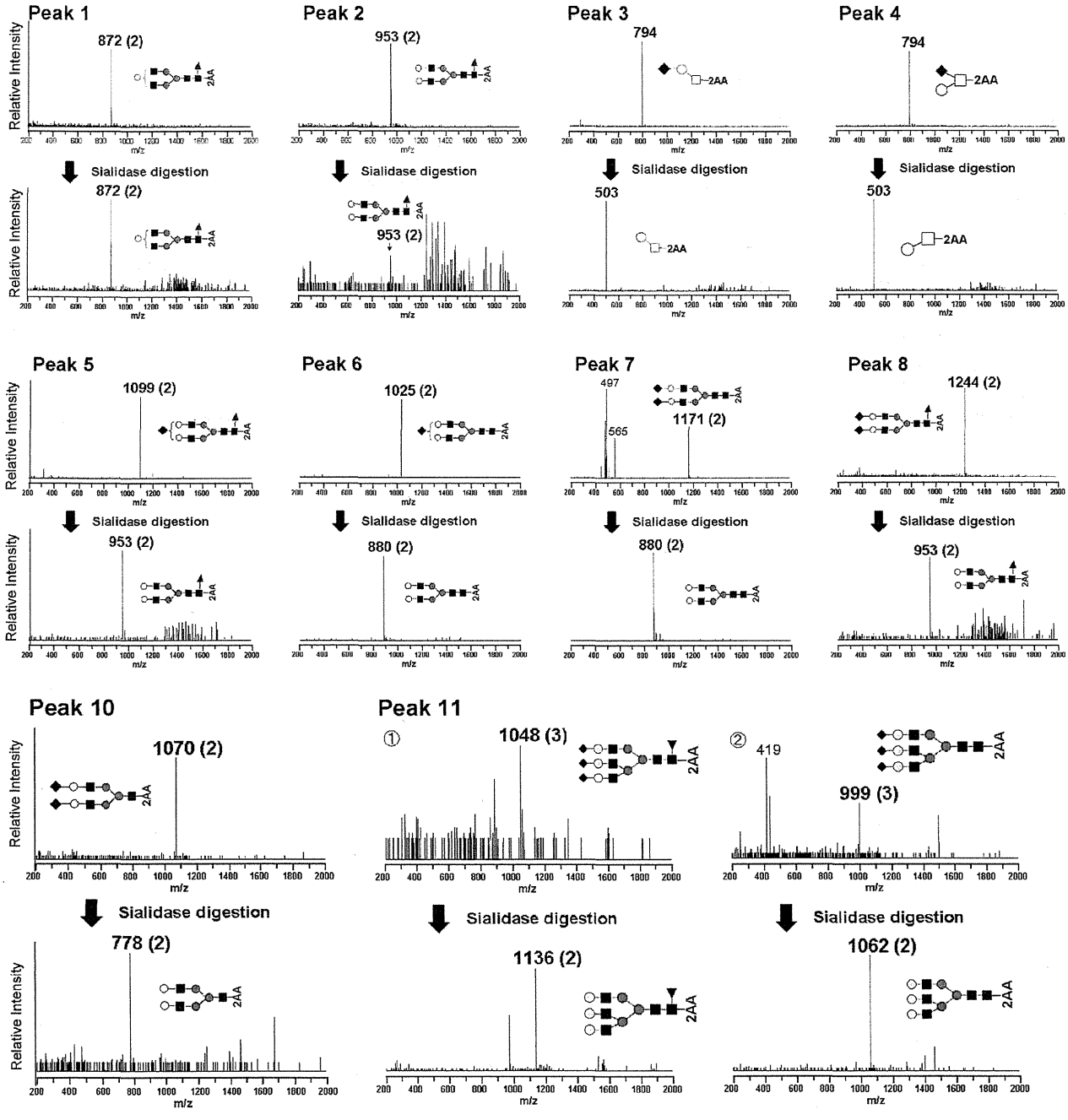

Fig. 3. ESI-IT-TOF mass spectra of peak 1–8, 10, 11 in Fig. 2. Symbols: triangles, fucose; others are the same as those in Fig. 1. Upper panels show the MS spectra of collected peaks. The collected peaks were digested with neuraminidase, and also analyzed by MS (lower panels).

the cytosolic ENGase (endo-β-N-acetylglucosaminidase) [22,23] or chitobiase [24]. It should be noted that most free glycans found in the present study bear N-acetylchitobiose structure other than peak **10**. Kimura et al. reported that free glycans were accumulated not only inside cells but also secreted to the extracellular space in rice cell culture [25,26]. In addition, they suggested that the extracellular acidic peptide N-glycanase was involved in accumulation of such glycans. We have to also consider the presence of free O-glycans (**3** and **4**), although the amounts of these glycans are quite small.

The mechanism of the presence/formation of free glycans in sera and the source of these glycans are not clear in the present study. However, it is quite interesting if these glycans are varied with physiological changes.

4. Conclusions

The present study demonstrates that free glycans exist in human serum. Most of the glycans were sialic acid-containing complex-type glycans. Of the glycans, disialo-biantennary glycan which does

not carry fucose residue is present most abundantly. And high mannose-type glycans were not detected at all. From these results, we suppose that these free glycans were due to glycoproteins in sera, although further studies are required.

References

[1] D. Kmiecik, V. Herman, C.J. Stoop, A.M. Mir, O. Labiau, A. Verbert, Glycobiology 5 (1995) 483.
[2] K. Yanagida, S. Natsuka, S. Hase, Glycobiology 16 (2006) 294.
[3] T. Suzuki, H. Park, W.J. Lennarz, FASEB J. 16 (2002) 635.
[4] I. Chantret, S.E. Moore, Glycobiology 18 (2008) 210.
[5] T. Suzuki, Y. Funakoshi, Glycoconj. J. 23 (2006) 291.
[6] D.J. Kelleher, R. Gilmore, Glycobiology 16 (2006) 47R.
[7] T. Suzuki, Semin Cell, Dev. Biol. 18 (2007) 762.
[8] R. Naka, S. Kamoda, A. Ishizuka, M. Kinoshita, K. Kakehi, J. Proteome Res. 5 (2006) 88.
[9] A. Ishizuka, Y. Hashimoto, R. Naka, M. Kinohita, K. Kakehi, J. Seino, Biochem. J. 413 (2008) 227.
[10] Y. Matsuno, K. Yamada, A. Tanabe, M. Kinoshita, S. Maruyama, Y. Osaka, T. Masuko, K. Kakehi, Anal. Biochem. 362 (2007) 245.
[11] K. Yamada, S. Hyodo, Y. Matsuno, M. Kinoshita, S. Maruyama, Y. Osaka, E. Casal, Y.C. Lee, K. Kakehi, Anal. Biochem. 371 (2007) 52.
[12] K. Yamada, M. Kinoshita, T. Hayakawa, S. Nakaya, K. Kakehi, J. Proteome Res. 8 (2009) 521.
[13] K. Yamada, S. Hyodo, M. Kinoshita, T. Hayakawa, K. Kakehi, Anal. Chem. 82 (2010) 7436.
[14] B. Winchester, Glycobiology 15 (2005) 1R.
[15] J.C. Michalski, J. Lemone, J.M. Wieruszeski, B. Fournet, J. Montreuil, G. Strecker, Eur. J. Biochem. 198 (1991) 521.
[16] G. Strecker, M.C. Peers, J.C. Michalski, T. Hondi-Assah, B. Fournet, G. Spik, J. Montreuil, J.P. Farriaux, P. Maroteaux, P. Durand, Eur. J. Biochem. 75 (1977) 391.
[17] J. van Pelt, K. Hard, J.P. Kamerking, J.F. Vliegenthart, A.J. Reuser, H. Galjaard, Biol. Chem. Hoppe-Seyler 370 (1989) 191.
[18] K. Ishii, M. Iwasaki, S. Inoue, P.T.M. Kenny, H. Komura, Y. Inoue, J. Biol. Chem. 264 (1989) 1623.
[19] M. Tajiri, C. Ohyama, Y. Wada, Glycobiology 18 (2008) 2.
[20] G. Weisshaar, J. Hiyama, A.G.C. Renwick, Glycobiology 1 (1991) 393.
[21] L. Sturiale, R. Barone, A. Fiumara, M. Perez, M. Zaffanello, G. Sorge, L. Pavone, S. Tortorelli, J.F. O'Brien, J. Jaeken, D. Garozzo, Glycobiology 15 (2005) 1268.
[22] T. Kato, K. Hatanaka, T. Mega, S. Hase, J. Biochem. 122 (1997) 1167.
[23] T. Suzuki, K. Yano, S. Sugimoto, K. Kitajima, W.J. Lennarz, S. Inoue, Y. Inoue, Y. Emori, Proc. Natl. Acad. Sci. U.S.A. 99 (2002) 9691.
[24] R. Cacan, C. Dengremont, O. Labiau, D. Kmiecik, A. Mir, A.M. Verbert, J. Biochem. 313 (1996) 597.
[25] Y. Kimura, S. Matsuo, J. Biochem. 127 (2000) 1013.
[26] M. Maeda, M. Kimura, Y. Kimura, J. Biochem. 148 (2010) 681.

Structures of Two New Phenolic Glycosides, Kaempferiaosides A and B, and Hepatoprotective Constituents from the Rhizomes of *Kaempferia parviflora*

Saowanee Chaipech,[a] Toshio Morikawa,*[,a] Kiyofumi Ninomiya,[a] Masayuki Yoshikawa,[a] Yutana Pongpiriyadacha,[b] Takao Hayakawa,[a] and Osamu Muraoka[a]

[a] *Pharmaceutical Research and Technology Institute, Kinki University; 3–4–1 Kowakae, Higashi-osaka, Osaka 577–8502, Japan: and* [b] *Faculty of Science and Technology, Rajamangala University of Technology Srivijaya; Thungsong, Nakhonsithammarat 80110, Thailand.*

Received August 20, 2011; accepted October 4, 2011; published online October 13, 2011

Two new phenolic glycosides, kaempferiaosides A and B were isolated from the rhizomes of *Kaempferia parviflora* (Zingiberaceae) together with 24 known compounds. Their structures including absolute stereochemistry were elucidated on the basis of chemical and spectroscopic evidence. Among the isolates, 5,3′-dihydroxy-3,7,4′-trimethoxyflavone showed higher activity than silybin, a commercial hepatoprotective agent.

Key words *Kaempferia parviflora*; Zingiberaceae; kaempferiaoside; hepatoprotective activity; Krachai Dum

A Zingiberaceae plant, *Kaempferia parviflora* WALL. *ex* BAKER, is widely distributed in Thailand and is known as Krachai Dum.[1,2] The rhizomes of this plant are tinged with-dark purple to black, and have traditionally been used for the treatment of hypertension,[3—5] allergy,[6] gastrointestinal disorders,[7] and impotence.[8,9] The extract of the rhizomes of *K. parviflora* and its constituents were revealed to exhibit several pharmacological activities, such as antiplasmoidal, antifungal,[2] anti-inflammatory,[10—12] α-glucosidase inhibitory,[13] and xanthine oxidase inhibitory[1] activities and cytotoxicity of several tumor cell lines[14,15] as well as effect of P-glycoprotein function[16] and modulation of multi-drug resistance in cancer cells.[17] Recently, rhizomes of *K. parviflora* powder was found to show preventive effect from obesity and its downstream symptoms.[18] By a previous chemical study on *K. parviflora*, presence of several methoxyflavones and related phenolic constituents have been revealed.[2,5,6,10—15,17,19—22] During the course of our characterization studies on Thai natural medicines,[23—32] two new phenolic glycosides named kaempferiaosides A (**1**) and B (**2**) were isolated from the rhizomes of *K. parviflora* together with 24 known compounds. This paper deals with the structure elucidation of **1** and **2**, as well as hepatoprotective effect of the constituents from the rhizomes of *K. parviflora* on D-galactosamine (D-GalN)-induced cytotoxicity in primary cultured mouse hepatocytes.

The dried rhizomes of *K. parviflora* cultivated at Loei province, Thailand were extracted with methanol to give a methanolic extract (7.10% from the dried rhizomes). The methanolic extract was partitioned into an EtOAc–H_2O (1 : 1, v/v) mixture to furnish an EtOAc-soluble fraction (3.82%) and an aqueous phase. The aqueous phase was subjected to Diaion HP-20 column chromatography ($H_2O \rightarrow$ MeOH) to give H_2O- and MeOH-eluted fractions (2.04, 1.23%, respectively). As shown in Table 1, the EtOAc-soluble fraction and the MeOH-eluted fraction exhibited hepatoprotective activity, but the H_2O-eluted fraction lacked the activity. The EtOAc-soluble fraction was subjected to normal- and reversed-phase column chromatographies, and finally HPLC to give 5-hydroxy-7-methoxyflavone[33] (**3**, 0.113%), 5,7-dimethoxyflavone[19,22] (**4**, 0.549%), 5,4′-dihydroxy-7-methoxyflavone[33] (**5**, 0.0028%), 5-hydroxy-7,4′-dimethoxyflavone[20] (**6**, 0.066%), 5,7,4′-trimethoxyflavone[20] (**7**, 0.838%), 5-hydroxy-7,3′,4′-trimethoxyflavone[34] (**8**, 0.00048%), 5,7,3′,4′-tetramethoxyflavone[20] (**9**, 0.096%), 5-hydroxy-3,7-dimethoxyflavone[20] (**10**, 0.151%), 3,5,7-trimethoxyflavone[20] (**11**, 0.087%), 5-hydroxy-3,7,4′-trimethoxyflavone[20] (**12**, 0.211%), 3,5,7,4′-tetramethoxyflavone[20] (**13**, 0.296%), 5,3′-dihydroxy-3,7,4′-trimethoxyflavone[19,35] (**14**, 0.028%), 5-hydroxy-3,7,3′,4′-tetramethoxyflavone[20] (**15**, 0.046%), 3,5,7,3′,4′-pentamethoxyflavone[19,20] (**16**, 0.745%), and (2*R*,3*R*)-(−)-aromadendrin trimethyl ether[36] (**17**, 0.0010%). From the MeOH-eluted fraction, **1** (0.0026%), **2** (0.00050%), tilianine[37] (**18**, 0.0015%), tamarixetin 3-*O*-rutinoside[38] (**19**, 0.00035%), syringetin 3-*O*-rutinoside[39] (**20**, 0.00054%), (2*R*,3*S*,4*S*)-3-*O*-[α-L-rhamnopyranosyl-(1 → 6)-β-D-glucopyranosyl]-3′-*O*-methyl-*ent*-epicatechin-(2α → *O* → 3,4α → 4)-(5a*S*,10b*S*)-5a,10b-dihydro-1,3,5a,9-tetrahydroxy-8-methoxy-6*H*-benz[*b*]indeno[1,2-*d*]furan-6-one 5a-*O*-[α-L-rhamnopyranosyl-(1 → 6)-β-D-glucopyranoside][21] (**21**, 0.0044%), *rel*-(5a*S*,10b*S*)-5a,10b-dihydro-1,3,5a,9-tetrahydroxy-8-methoxy-6*H*-benz[*b*]indeno[1,2-*d*]furan-6-one 5a-*O*-[α-L-rhamnopyranosyl-(1 → 6)-β-D-glucopyranoside][21] (**22**, 0.012%), *rel*-(5a*S*,10b*R*)-5a,10b-dihydro-1,3,5a,9-tetrahydroxy-8-methoxy-6*H*-benz[*b*]indeno[1,2-*d*]furan-6-one 5a-*O*-[α-L-rhamnopyranosyl-(1 → 6)-β-D-glucopyranoside][21] (**23**, 0.0040%), 2,4,6-trihydroxyacetophenone 2,4-di-*O*-β-D-glucopyranoside[40] (**24**, 0.00043%), adenosine[41] (0.00080%), and L-phenylalanine[41] (0.00070%) were isolated by normal- and reversed-phase column chromatographies, and finally HPLC.

Structures of Kaempferiaosides A (1) and B (2) Kaempferiaoside A (**1**) was obtained as an amorphous powder with negative optical rotation ($[\alpha]_D^{23}$ −153.8° in MeOH). In the positive-ion fast atom bombardment (FAB)-MS of **1**, a quasimolecular ion peak was observed at *m/z* 1285 $(M+Na)^+$, and high-resolution positive-ion FAB-MS analysis revealed the molecular formula of **1** to be $C_{57}H_{66}O_{32}$. The IR spectrum of **1** showed absorption bands at 1624, 1458, and 1225 cm^{-1} ascribable to aromatic ring, and broad bands at 3400 and 1069 cm^{-1}, suggestive of a glycosyl moiety. Acid hydrolysis of **1** with 1.0 M hydrochloric acid liberated L-rhamnose and D-glucose, which were identified by HPLC using an optical

* To whom correspondence should be addressed. e-mail: morikawa@kindai.ac.jp

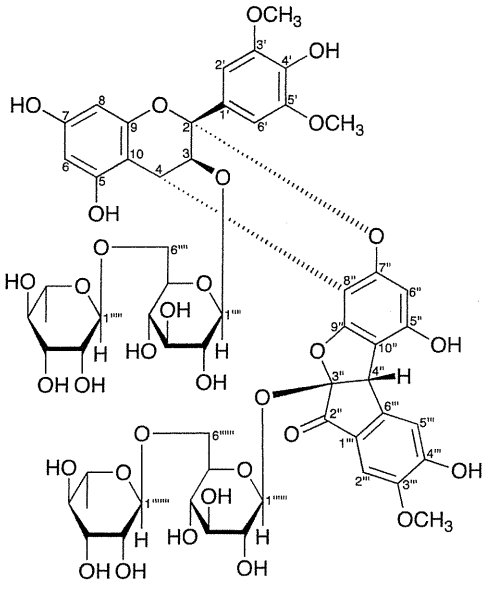

Kaempferiaoside A (**1**)

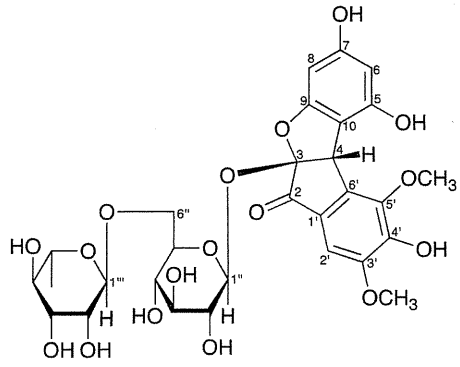

Kaempferiaoside B (**2**)

Chart 1

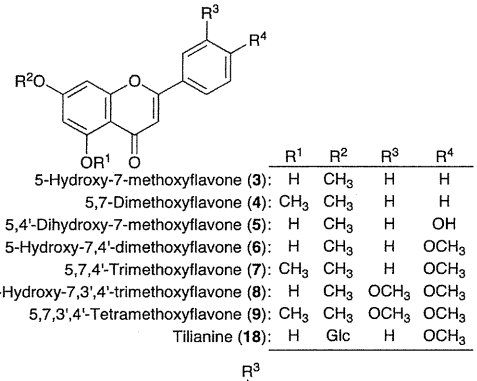

	R^1	R^2	R^3	R^4
5-Hydroxy-7-methoxyflavone (**3**):	H	CH_3	H	H
5,7-Dimethoxyflavone (**4**):	CH_3	CH_3	H	H
5,4'-Dihydroxy-7-methoxyflavone (**5**):	H	CH_3	H	OH
5-Hydroxy-7,4'-dimethoxyflavone (**6**):	H	CH_3	H	OCH_3
5,7,4'-Trimethoxyflavone (**7**):	CH_3	CH_3	H	OCH_3
5-Hydroxy-7,3',4'-trimethoxyflavone (**8**):	H	CH_3	OCH_3	OCH_3
5,7,3',4'-Tetramethoxyflavone (**9**):	CH_3	CH_3	OCH_3	OCH_3
Tilianine (**18**):	H	Glc	H	OCH_3

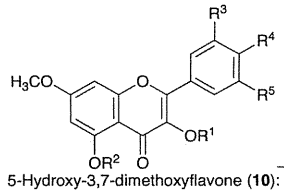

	R^1	R^2	R^3	R^4	R^5
5-Hydroxy-3,7-dimethoxyflavone (**10**):	CH_3	H	H	H	H
3,5,7-Trimethoxyflavone (**11**):	CH_3	CH_3	H	H	H
5-Hydroxy-3,7,4'-trimethoxyflavone (**12**):	CH_3	H	H	OCH_3	H
3,5,7,4'-Tetramethoxyflavone (**13**):	CH_3	CH_3	H	OCH_3	H
5,3'-Dihydroxy-3,7,4'-trimethoxyflavone (**14**):	CH_3	H	OH	OCH_3	H
5-Hydroxy-3,7,3',4'-tetramethoxyflavone (**15**):	CH_3	H	OCH_3	OCH_3	H
3,5,7,3',4'-Pentamethoxyflavone (**16**):	CH_3	CH_3	OCH_3	OCH_3	H
Tamarixetin 3-*O*-rutinoside (**19**):	$Rha^1—^6Glc$	H	OH	OCH_3	H
Syringetin 3-*O*-rutinoside (**20**):	$Rha^1—^6Glc$	H	OCH_3	OH	OCH_3

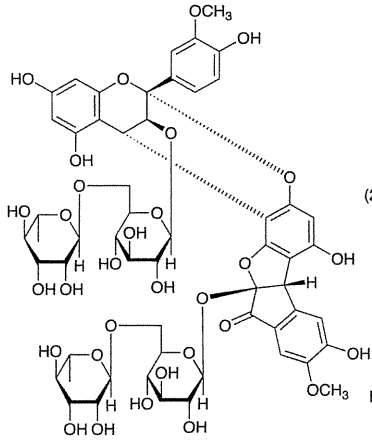

21

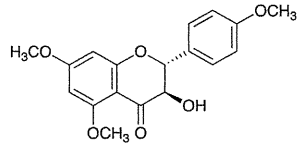

(2*R*,3*R*)-(−)-Aromadendrin trimethyl ether (**17**)

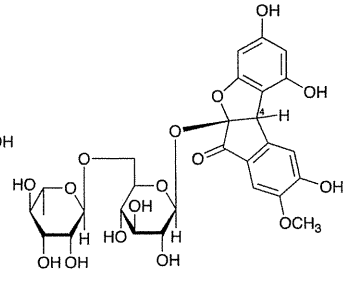

22: 4β-H
23: 4α-H

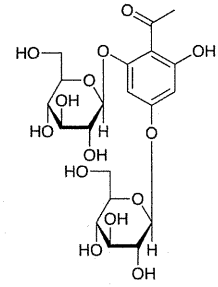

2,4,6-Trihydroxyacetophenone
2,4-di-*O*-β-D-glucopyranoside (**24**)

Glc: β-D-glucopyranosyl
Rha: α-L-rhamnopyranosyl

Chart 2

rotation detector.[42] The ^{1}H- and ^{13}C-NMR spectra (CD_3OD, Table 2) of **1**, which were assigned by various NMR experiments,[43] showed signals assignable to three methoxy groups [δ 3.50 (3H, brs, 3‴-OCH_3), 3.89 (6H, s, 3′,5′-OCH_3)], three methines [δ 4.53, 4.93 (1H each, both d, J=3.5 Hz, 3, 4-H), 5.33 (1H, brs, 4″-H)], and seven aromatic protons [δ 5.82, 5.83 (1H each, d, J=2.3 Hz, 8, 6-H), 6.18 (1H, s, 6″-H), 7.01 (3H, s, 2′,6′, 2‴-H), 7.32 (1H, brs, 5‴-H)] together with two

Table 1. Inhibitory Effects of the Methanolic Extract from the Rhizomes of *K. parviflora* and Its Fractions on D-GalN-Induced Cytotoxicity in Primary Cultured Mouse Hepatocytes

	Inhibition (%)				
	0 μg/mL	3 μg/mL	10 μg/mL	30 μg/mL	100 μg/mL
MeOH extract	0.0±1.9	11.5±0.6**	18.4±1.3**	16.1±1.7**	—
EtOAc-soluble fraction	0.0±2.6	12.4±2.1**	23.3±2.3**	—	—
MeOH-eluted fraction	0.0±1.4	4.4±0.3	10.4±1.3**	19.6±1.7**	42.5±2.6**
H_2O-eluted fraction	0.0±2.7	−0.8±0.7	−1.9±0.9	−2.1±1.4	2.2±2.3

Each value represents the mean±S.E.M. (n=4). Significantly different from the control, **p<0.01.

Table 2. ^{1}H-NMR (500 MHz) and ^{13}C-NMR (125 MHz) Data for **1**

Position	δ_H (J Hz)	δ_C	Position	δ_H (J Hz)	δ_C
2		100.1	3-*O*-Glc		
3	4.53 (1H, d, 3.5)	70.1	1''''	4.57 (1H, d, 7.5)	99.7
4	4.93 (1H, d, 3.5)	25.0	2''''	2.98 (1H, dd, 7.5, 9.2)	75.3
5		156.5	3''''	3.57 (1H, m)	77.3
6	5.83 (1H, d, 2.3)	97.5	4''''	3.12 (1H, dd like)	71.9
7		158.6	5''''	3.48 (1H, m)	77.2
8	5.82 (1H, d, 2.3)	95.4	6''''	3.48 (1H, m)	68.3
9		154.1		3.92 (1H, m)	
10		105.4	6''''-*O*-Rha		
1'		131.0	1'''''	4.66 (1H, br s)	102.4
2',6'	7.01 (2H, s)	106.2	2'''''	3.71 (1H, m)	72.2
3',5'		148.5	3'''''	3.58 (1H, m)	72.4
4'		137.1	4'''''	3.31 (1H, m)	74.0
2'		195.7	5'''''	3.55 (1H, m)	69.9
3'		113.0	6'''''	1.18 (3H, d, 6.3)	18.0
4'	5.33 (1H, br s)	49.4	3'-*O*-Glc		
5''		154.1	1''''''	4.72 (1H, d, 7.8)	99.4
6''	6.18 (1H, s)	97.6	2''''''	3.35 (1H, m)	75.5
7''		155.1	3''''''	3.68 (1H, m)	76.5
8''		100.2	4''''''	3.36 (1H, m)	71.2
9''		158.6	5''''''	3.31 (1H, m)	76.5
10''		107.4	6''''''	3.52 (1H, m)	67.2
1'''		124.5		3.93 (1H, m)	
2'''	7.01 (1H, s)	106.4	6''''''-*O*-Rha		
3'''		150.7	1'''''''	4.67 (1H, br s)	101.9
4'''		158.6	2'''''''	3.94 (1H, m)	72.2
5'''	7.32 (1H, br s)	113.8	3'''''''	3.71 (1H, m)	72.4
6'''		152.5	4'''''''	3.34 (1H, m)	74.2
3',5'-OCH_3	3.89 (6H, s)	57.1	5'''''''	3.65 (1H, m)	69.7
3'''-OCH_3	3.50 (3H, br s)	56.1	6'''''''	1.24 (3H, d, 6.3)	18.1

Measured in CD_3OD.

rhamnopyranosyl [δ 1.18 (3H, d, J=6.3 Hz, 6''''-H_3), 1.24 (3H, d, J=6.3 Hz, 6'''''-H_3), 4.66, 4.67 (1H each, both br s, 1'''', 1'''''-H)] and two glucopyranosyl moieties [δ 4.57 (1H, d, J=7.5 Hz, 1''''-H), 4.72 (1H, d, J=7.8 Hz, 1'''''-H)]. As shown in Fig. 1, the ^{1}H–^{1}H correlation spectroscopy (COSY) experiments on **1** indicated the presence of three partials written in bold lines. In the heteronuclear multiple bond connectivity (HMBC) experiment, long range correlations were observed between the following proton and carbon pairs: 3-H and 2-C; 4-H and 2, 9, 10, 8'', 9''-C; 6-H and 8, 10-C; 8-H and 6, 10-C; 2',6'-H and 2, 4'-C; the 3',5'-methoxy methyl protons and 3',5'-C; 4''-H and 3'', 5'', 9'', 10'', 1''', 6'''-C; 6''-H and 8'', 10''-C; 2'''-H and 4''', 6'''-C; 5'''-H and 1''', 3'''-C; the 3'''-methoxy proton and 3'''-C; 1''''-H and 3-C; 1''''-H and 6''''-C; 1'''''-H and 3''-C; 1'''''-H and 6'''''-C (Fig. 1). The proton and carbon signals in the ^{1}H- and ^{13}C-NMR spectra of **1** were similar to those of **21**, except for the signals due to the B ring in the flavan-3-ol unit. The relative stereochemistry of **1** was determined on the basis of the coupling constants in the ^{1}H-NMR spectrum and the rotating frame nuclear Overhauser effect spectroscopy (ROESY) experiment. The 2,3-*trans* form in the flavan-3-ol unit was identified by comparison of the coupling constant ($J_{3,4}$=3.5 Hz) with that of **21** ($J_{3,4}$=3.7 Hz).[21] The rotating frame Overhauser effect (ROE) correlations were observed between following proton pairs: 6-H and 2'''-H; 2',6'-H and 3',5'-OCH_3; 2'''-H and the 3'''-OCH_3; and 4''-H and 1'''''-H (Fig. 1). Finally, the absolute stereochemistry of **1** was elucidated by circular dichroism (CD) spectrum, which showed a negative Cotton effect in the

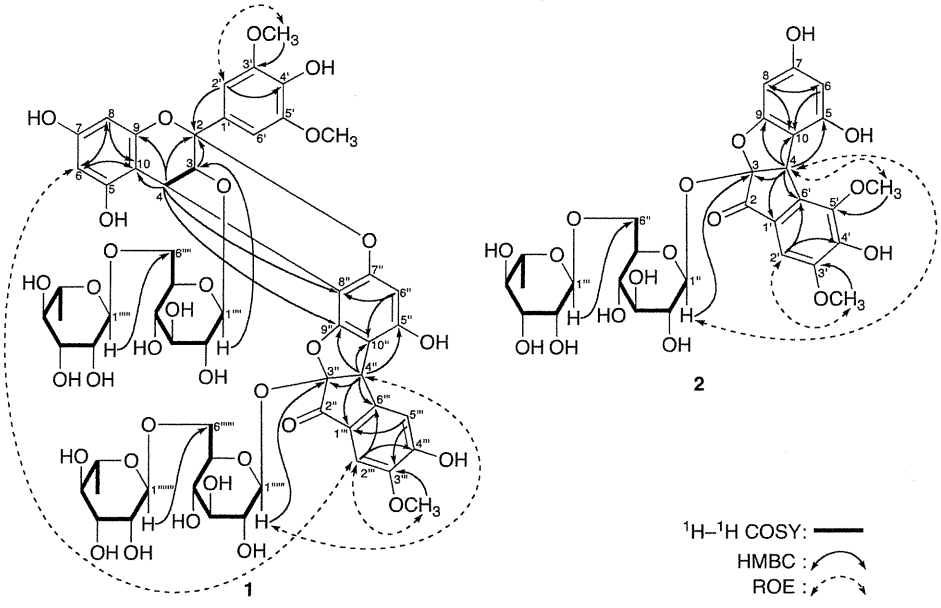

Fig. 1. ^{1}H–^{1}H COSY, HMBC, and NOESY Correlations for **1** and **2**

Table 3. ^{1}H-NMR (700 MHz) and ^{13}C-NMR (175 MHz) Data for **2**

Position	δ_H (*J* Hz)	δ_C	Position	δ_H (*J* Hz)	δ_C
2		194.9	3-*O*-Glc		
3		112.1	1″	4.57 (1H, d, 7.4)	99.2
4	5.01 (1H, s)	45.1	2″	3.02 (1H, m)	73.3
5		154.2	3″	3.11 (1H, m)	76.9
6	5.83 (1H, d, 2.0)	96.7	4″	3.11 (1H, m)	69.2
7		159.4	5″	2.98 (1H, m)	75.8
8	5.79 (1H, d, 2.0)	89.4	6″	3.39 (1H, m)	66.3
9		160.2		3.68 (1H, dd, 2.1, 11.0)	
10		103.8	6″-*O*-Rha		
1′		123.5	1‴	4.52 (1H, d, 1.9)	100.9
2′	6.89 (1H, s)	102.0	2‴	3.65 (1H, m)	70.4
3′		152.0	3‴	3.41 (1H, m)	70.8
4′		148.5	4‴	3.16 (1H, m)	72.2
5′		142.7	5‴	3.39 (1H, m)	68.4
6′		139.1	6‴	1.07 (3H, d, 6.2)	17.8
3′-OCH_3	3.76 (3H, s)	56.0			
5′-OCH_3	3.90 (3H, s)	60.3			

Measured in DMSO-d_6.

short wavelength region ($\Delta\varepsilon$ −37.54 at 214 nm), indicating that the orientation of the 4-position in the flavan-3-ol unit is *S* configuration.[21,44–47] This evidence indicated that the absolute configuration of **1** was determined to be 2*R*, 3*S*, 4*S*, 3″*S*, and 4″*S* orientations. Consequently, the absolute stereostructure of **1** was determined to be as shown.

Kaempferiaoside B (**2**) was also obtained as an amorphous powder with negative optical rotation ($[\alpha]_D^{23}$ −166.8° in MeOH). The molecular formula, $C_{29}H_{34}O_{17}$, of **2** was determined by high-resolution positive-ion FAB-MS measurement. Acid hydrolysis of **2** with 1 M HCl liberated L-rhamnose and D-glucose, which were identified by HPLC using an optical rotation detector. The proton and carbon signals in the ^{1}H- and ^{13}C-NMR spectra (DMSO-d_6, Table 3) of **2** were superimposable on those of **22**, except for the signals due to an additional 5′-methoxy group: two methoxy groups [δ 3.76, 3.90 (3H each, both s, 3′, 5′-OCH_3)], a methine [δ 5.01 (1H, s, 4-H)], and three aromatic protons [δ 5.79, 5.83 (1H each, d, *J*=2.0 Hz, 8, 6-H), 6.89 (1H, s, 2′-H)] together with a rhamnopyranosyl [δ 1.07 (3H, d, *J*=6.2 Hz, 6‴-H_3), 4.52 (1H, d, *J*=1.9 Hz, 1‴-H)] and a glucopyranosyl moieties [δ 4.57 (1H, d, *J*=7.4 Hz, 1″-H)]. In the HMBC experiment on **2**, long-range correlations were observed between the following protons and carbons: 4-H and C-3, 5, 9, 10, 1′, 6′-C; 6-H and 8, 10-C; 8-H and 6, 10-C; 2′-H and 4′, 6′-C; the 3′-methoxy proton and 3′-C; the 5′-methoxy proton and 5′-C; 1″-H and 3-C; 1‴-H and 6″-C (Fig. 1). The ROE correlations were observed as shown in Fig. 1 (4-H, 1″-H, 5′-methoxy proton; 2′-H, 3′-methoxy proton). Consequently,